Closed-loop identification using finite data

van den Broek, J.R.M.

Award date:
1997

Technische Universiteit Eindhoven

Faculteit Technische
Natuurkunde
Vakgroep Systeem-
en Regeltechniek
Gebouw W&S
Postbus 513
5600 MB Eindhoven

Title: **Closed-loop Identification Using Finite Data**

Author: J.R.M. van den Broek

Report number: NR-1975

Date: May 20, 1997

ÉCOLE POLYTECHNIQUE
FÉDÉRALE DE LAUSANNE

INSTITUT
D'AUTOMATIQUE

Département Génie
Mécanique
Institut
d'Automatique
CH 1015
Lausanne

Institut d'automatique (IA)

CH - 1015 Lausanne (Switzerland)
Tél. : (+41) (21) 693 38 45 Fax : (+41) (21) 693 25 74

ÉCOLE POLYTECHNIQUE
FÉDÉRALE DE LAUSANNE

Lausanne, le 26 septembre 1996

Travail pratique de diplôme
Hiver 1996

Candidat : **Joost VAN DEN BROEK - (ERASMUS)**
Technische Universiteit TU Eindhoven

Sujet : **Closed-loop identification using finite data**

Closed-loop identification gives usually more appropriate model for the controller design. One reason is that the input spectrum is automatically adjusted to the frequency range of interest. Another reason is that larger control signals can then be used for e.g. resonant systems. Then, e.g. dry friction effects on the estimated model become less important. The existing theory requires infinite data records for the validity of asymptotic results. This project is concerned with evaluation of various closed-loop identification schemes when only finite data is available.

Prof. D. Bonvin

Assistant : Ulf HOLMBERG (tél. interne : 3830)

Summary

The design of high performance controllers for a specific process is usually based on a model of the process. An analytical approach, using basic laws from physics and chemistry may lead to a complex, high order model that is not appropriate for the controller design. An alternative approach is system identification. This approach uses experimentally obtained data to fit the parameters of a certain model. With respect to this *identification for control* problem it has been established that the data obtained from a closed-loop identification experiment usually give a better model for the controller design.
It is therefore necessary to study closed-loop identification. This report examines different methods that can tackle the closed-loop identification problem. It includes a study on the general properties of identification and on the identification objective. Recently developed methods are examined theoretically and by an application to a magnetic levitation process. A Labview visual interface has been built to control this process and to collect data. A special interface has been implemented to make data exchange with Matlab possible. This interface allows the use of user defined input signals, that are created in the Matlab environment, in the experimental setup that is supervised by the Labview interface.
The success of an identification experiment depends heavily on the input signal. A study of different input signals led to the conclusion that multisines are appropriate input signals for an identification experiment. They allow full control over the order of excitation and they can be optimized to the information density.
Any identification experiment should be followed by a validation. In this report, different types of validation are examined. This overview includes statistical validation methods as well as methods that are directed towards the control objective.
Special attention is being paid to this control objective of identification. A scheme that iteratively performs an identification and a controller design is included in the report. This scheme was applied to a simulated system as well as to the laboratorium experiment.
The experiments led to an important conclusion. All identification schemes as well as the identification for control scheme needed a data filter to perform successfully. A method to construct this filter from closed-loop data has been developed and was applied successfully in the identification of the magnetic levitation.

Preface

This report is the result from a nine months scientific stage I did at the Ecole Polytechnique Fédérale de Lausanne, at the Institut d'Automatique.
I would like to thank the members of the institute who helped me during my stay and with whom I spend a great time at the institute. In particular, I would like to thank Ulf, my mentor, for helping me with all sorts of problems and all the support he gave me. I owe a lot to Olivier, who was of great help during my experiments with the magnetic levitation process and Christophe for helping me out of all kinds of software problems I encountered. Further, I would like to thank prof. Bonvin and prof. Preisig for their support during the project.
This stage would not have been possible without the support from the both the University of Eindhoven and the EPFL. I would like to thank the Bureau of Foreign Affairs from the University of Eindhoven and the Service Academique of the EPFL.

Contents

I

Introduction

1.1 Backgrounds

Many industrial processes must be controlled to operate safely and efficiently. To design high performance controllers a model of the process to be controlled is needed. These models can be derived in different ways. An analytical approach, using basic laws from physics and chemistry, leads to a mathematical model of the process under consideration. This procedure often results in a very detailed description of all the individual phenomena governing the behaviour of the system, leading to a complex high order model. But in many cases the processes are so complex that it is not possible to find a reasonable model that explains the behaviour of the system. An alternative approach is system identification. This approach uses experimentally obtained data to fit the parameters of a certain model. In contrast to analytically obtained models they are relatively easy to use but they have only limited validity and they give little physical insight.
One of the objectives of an identification experiment is the derivation of an appropriate model for model-based control design. An interrelation between these fields of research can thus be expected. However, these relations have been developed only recently. On the one hand, the objective of identification was mainly the reconstruction of the 'real' plant. On the other hand model-based control developed into robust control, taking into account that an estimated model is not necessarily a perfect description of the process. At the end of the eighties some first attempts were made to bring identification and control together. This led to a new area of research: *identification for control.*
Within the latter context, it has been established that identification performed in a closed-loop setup usually gives a more appropriate model for the controller design. One reason is that the input spectrum is automatically adjusted to the frequency range of interest. Another reason is that larger control signals can then be used for e.g. resonant systems. A third motivation to study closed-loop identification is the fact that sometimes it is not at all possible to perform an open-loop experiment. The open-loop system may be unstable or poorly damped or there may be practical restrictions from e.g. a safety point of view. This report will concentrate on closed-loop identification and touch the subject of identification for control. However, emphasis will be put on the identification problem.

1.2 Outline

A typical identification experiment consists of different parts. Chapter two will outline the general concepts of identification. The problem of identifiability will be considered and an

analysis of the properties of both open-loop and closed-loop identification will be given. By means of an example it will be shown that closed-loop identification can give better results than an open-loop one. But before any identification experiment can be performed an input signal must be selected. The third chapter will treat this problem. The fourth chapter will discuss different methods of validation. Any identification experiment should always be followed by a validation in order to determine the quality of the obtained estimates. Chapter five discusses some methods for closed-loop identification. Not only schemes for identification will be treated, but also a scheme that combines the identification with a controller design in an iterative way. A benchmark example is chosen for comparison and evaluation of the different methods. In chapter six a 'real life' identification experiment will be presented, and the relation between identification and control will be shown by the application of an iterative scheme in which identification and controller design are alternated in order to arrive at a high performance controller.

II

Identification

In this chapter the general concepts of identification will be introduced. The first section will give some definitions of the concepts that will be used later. The prediction error framework will be discussed in the second section and problems of identifiability and uniqueness will be treated in the third. These concepts can be used to analyze the properties of the so-called classical identification methods. This analysis will show the need for a new approach for the closed-loop identification problem. Some first examples of validation methods, that will be discussed in more detail later, are given in the last two sections. Both a statistical validation and a validation towards a control objective will be treated.

2.1 General concepts

The result of an identification experiment depends on four concepts: *the system, the model structure, the identification method and the experimental condition.* These concepts will be used throughout this report and are therefore defined below. A block diagram of a general system is given in Figure 2.1.

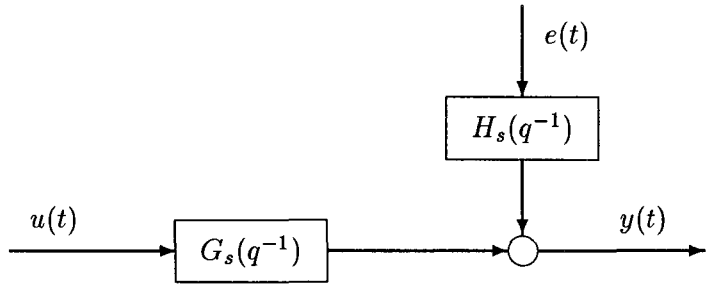

Figure 2.1: Block diagram of a system

Definition 2.1 *The system $\mathcal{S}$*
The system $\mathcal{S}$ is the physical reality that provides the experimental data. It includes a

deterministic part, the plant G_s, and a stochastic part H_s. A linear, time invariant, single input single output (SISO), discrete time system can be written as:

$$\mathcal{S}: \begin{cases} y(t) & = G_s(q^{-1})\, u(t) + H_s(q^{-1})\, e(t), \\ \mathrm{E}e(t)e(t') & = \Lambda_s\, \delta_{t,t'}, \end{cases} \tag{2.1}$$

where a white noise $e(t)$ enters through the dynamics H_s at the output $y(t)$. The input is denoted by $u(t)$. □

Definition 2.2 *The model structure $\mathcal{M}$*
When parametric models are considered, the model structure denotes a set of models that are characterized by a parameter vector θ:

$$\mathcal{M}: \begin{cases} y(t) & = G(q^{-1},\theta)\, u(t) + H(q^{-1},\theta)\, \epsilon(t), \\ \mathrm{E}\epsilon(t)\epsilon(t') & = \Lambda(\theta)\, \delta_{t,t'}, \end{cases} \tag{2.2}$$

where θ is varied over all parameter values, $\theta \in \Theta$. □

The model structure consists of two parts: a model for the plant and a model for the noise. These two parts are not necessarily parameterized independently. It is therefore convenient to define a set of plant models.

Definition 2.3 *Modelisation of the plant*
The set $\mathcal{P}$ consists of all possible modelisations of the plant:

$$\mathcal{P}: \{G(q^{-1},\theta) \mid \theta \in \Theta_p\}, \tag{2.3}$$

where, Θ_p is the parameter space containing all possible parameter vectors. □

In every identification experiment, the model structure must be chosen beforehand. Several factors should be taken into account when a model structure has to be determined. The structure must be flexible. It is important how the parameters enter the system and how many parameters are chosen. The latter consideration leads to the principle of *parsimony*: the model structure should contain the smallest number of free parameters to represent the system adequately. Typical structures are the output error structure, the ARX structure [1] and the Box-Jenkins structure.

Definition 2.4 *The identification method $\mathcal{I}$*
The identification method is the method that is used to identify the system under consideration. An identification method can be either parametric or nonparametric. □

Definition 2.5 *The experimental condition $\mathcal{H}$*
The experimental condition is a description of how the identification experiment has been done. It describes e.g. what signals are measured, how an input signal has been selected and generated and what sampling time has been used. □

[1] Autoregressive with an exogeneous signal. This structure is sometimes referred to as equation error structure.

From these definitions it is clear that only the system $\mathcal{S}$ is a property that can not be influenced. The experimental condition, the identification method and the model structure are 'parameters' that can be changed each identification experiment, and give the possibility to 'tune' the experiment towards a certain identification objective.

2.2 The prediction error framework

2.2.1 Model structure and predictor

Consider again the model (2.2). The one step ahead predictor depends on both the old inputs and the old outputs. It is defined by:

$$\hat{y}(t \mid t-1, \theta) \equiv H^{-1}(q^{-1}, \theta) G(q^{-1}, \theta) u(t) + [1 - H^{-1}(q^{-1}, \theta)] y(t). \tag{2.4}$$

The precise form of the predictor depends on the model structure that is used. The prediction error of output error and ARX model structures is discussed below.

Example 2.1 *One step ahead predictor*
ARX: The structure of an ARX model is the following:

$$\begin{aligned} \mathcal{M} : y(t) &+ a_1 y(t-1) + ... + a_{na} y(t-n_a) = b_1 u(t-1) + ... + b_{nb} u(t-n_b) + \epsilon(t) && (2.5) \\ &\Leftrightarrow A(q^{-1}) y(t) = B(q^{-1}) u(t) + \epsilon(t), && (2.6) \\ \theta &= [a_1, ..., a_{na}, b_1, ..., b_{nb}]^{\mathrm{T}}. && (2.7) \end{aligned}$$

The plant is thus modelled as $G(q^{-1}) = B(q^{-1})/A(q^{-1})$. The noise model is given by $A^{-1}(q^{-1})$. Analog to (2.4) the one step ahead predictor is:

$$\hat{y}(t \mid t-1, \theta) = [1 - A(q^{-1})] y(t) + B(q^{-1}) u(t). \tag{2.8}$$

OE: In an output error or OE model structure the noise model is equal to one. The model of the plant is $B(q^{-1})/F(q^{-1})$, where $F(q^{-1})$ is monic ($F(0) = 1$).

$$\begin{aligned} y(t) &= \frac{B(q^{-1})}{F(q^{-1})} u(t) + \epsilon(t), && (2.9) \\ \theta &= [b_1, ..., b_{nb}, f_1, ..., f_{nf}]^{\mathrm{T}}. && (2.10) \end{aligned}$$

The corresponding one step ahead predictor is:

$$\hat{y}(t \mid t-1, \theta) = \frac{B(q^{-1})}{F(q^{-1})} u(t). \tag{2.11}$$

□

2.2.2 Prediction error identification

The prediction error is defined as the difference between the output of the system and the one step ahead predictor at time t:

$$\varepsilon(t,\theta) \equiv y(t) - \hat{y}(t \mid t-1,\theta). \tag{2.12}$$

Using (2.1) and (2.4), this can be expanded to:

$$\varepsilon(t,\theta) = H^{-1}(q^{-1},\theta)[(G_s(q^{-1}) - G(q^{-1},\theta)u(t)] + H^{-1}(q^{-1},\theta)H_s(q^{-1})e(t). \tag{2.13}$$

The identification problem is now reduced to the minimization of the prediction error with regard to some criterion. For a least-squares (2-norm) criterion on the, possibly filtered, prediction errors the loss function is given by:

$$V_N(\theta) = \frac{1}{N}\sum_{t=1}^{N}\left[\varepsilon_f^2(t,\theta)\right], \tag{2.14}$$

$$\Rightarrow \hat{\theta}_N = \arg\min_{\theta\in\Theta} V_N(\theta). \tag{2.15}$$

where $\varepsilon_f(t,\theta) = L(q^{-1})\varepsilon(t,\theta)$, with $L(q^{-1})$ some stable prefilter. The number of data is denoted by N. For results on consistency, convergence and statistical properties of prediction error estimation is referred to [Söderström and Stoica (1989)]. Example 2.2 shows the computation of the prediction error estimate for an ARX model structure.

Example 2.2 *Prediction error identification for equation error structure*
Example 2.1 already introduced the parameter vector θ. If the measurements of the input and the output are collected in an *information vector* $\phi(t) = [-y(t-1),...,-y(t-na),u(t-1),...,u(t-nb)]^{\mathrm{T}}$ then the output of the model can be written as:

$$y(t) = \phi^{\mathrm{T}}\theta + \epsilon(t). \tag{2.16}$$

The residual $\epsilon(t)$ is linear in the parameters and a minimization of

$$V_N(\theta) = \frac{1}{N}\sum_{t=1}^{N}[y(t) - \phi^{\mathrm{T}}(t)\theta]^2 \tag{2.17}$$

has one unique solution given by

$$\hat{\theta} = \left[\frac{1}{N}\sum_{t=1} N\phi(t)\phi^{\mathrm{T}}(t)\right]^{-1}\left[\frac{1}{N}\sum_{t=1} N\phi(t)y(t)\right]. \tag{2.18}$$

In the case of an output error model structure the loss function is not linear in the parameters (see (2.9) and note that $\varphi(t)$ depends on θ through $\hat{y}(t-k,\theta)$, $k = 1,...,na$) leading to a nonlinear optimization problem that must be solved numerically. □

2.3 Identifiability and uniqueness

This section will introduce the concepts of identifiability and uniqueness. Identifiability will be introduced here in a general way, assuming a parametric model structure. Consider the system depicted in Figure 2.1.
Introduce a set $D_T(\mathcal{S},\mathcal{M})$ consisting of all parameter vectors for which the model structure $\mathcal{M}$ gives a perfect description of the system $\mathcal{S}$. Formally,

$$D_T(\mathcal{S},\mathcal{M}) = \{\theta \mid G_s(q^{-1}) \equiv G(q^{-1};\theta), H_s(q^{-1}) \equiv H(q^{-1};\theta), \Lambda_s = \Lambda(\theta)\}. \tag{2.19}$$

The following situations can occur:

$\mathcal{S} \in \mathcal{M}$ The system is a member of the set of models. There are two cases possible:

- The set $D_T(\mathcal{S},\mathcal{M})$ consists of several points. More than one parameter vector can describe the system perfectly. This situation is called overparametrization.
- The set $D_T(\mathcal{S},\mathcal{M})$ consists of exactly one point. A perfect description of the system is thus possible within the model structure. The parameter vector describing the system exactly will be denoted by θ_0.

$\mathcal{S} \notin \mathcal{M}$, **but** $G \in \mathcal{P}$ A perfect description of the plant can be given, but there is no perfect description of the noise.

$\mathcal{S} \notin \mathcal{M}$ The set $D_T(\mathcal{S},\mathcal{M})$ can be empty. This means that there is no perfect description of the system possible in the model structure $\mathcal{M}(\theta)$. This situation will be referred to as underparametrization.

Identifiablity can now be introduced using the concepts defined above.

Definition 2.6 *System identifiable*
The system $\mathcal{S}$ is system identifiable under $\mathcal{M},\mathcal{I},\mathcal{H}$ if

$$\hat{\theta}(N;\mathcal{S},\mathcal{M},\mathcal{I},\mathcal{H}) \to D_T(\mathcal{S},\mathcal{M}), \text{ as } N \to \infty, \tag{2.20}$$

(with probability one). Here, N denotes the number of measurements and $\hat{\theta}$ is the estimated parameter vector obtained from the application of an identification method $\mathcal{I}$ to the measurement data. □
Note, that, if the set $D_T(\mathcal{S},\mathcal{M})$ consists of more than one point, (2.20) should be interpreted as

$$\lim_{N\to\infty} \inf_{\theta \in D_T(\mathcal{S},\mathcal{M})} \| \hat{\theta}(N;\mathcal{S},\mathcal{M},\mathcal{I},\mathcal{H}) - \theta \| = 0. \tag{2.21}$$

Definition 2.7 *Parameter identifiable*
A system is parameter identifiable if it is system identifiable and the set $D_T(\mathcal{S},\mathcal{M})$ consists of exactly one point. □

2.3.1 Identifiability in open-loop

This subsection will pay attention to the concept of identifiability for systems that are operated in an open loop. Although the main issue in this report is closed-loop identification, it is important to know the properties of an open-loop identification as well. Especially since some of the closed-loop identification algorithms that will be discussed later in this report are based on a transformation from the closed-loop identification problem to an open-loop estimation problem. Consider the case where $\mathcal{S} \in \mathcal{M}$; the true system is in the set of models that is considered, or mathematically:

$$\exists \theta_0 : G(q^{-1}, \theta_0) = G_s(q^{-1}) \text{ and } H(q^{-1}, \theta_0) = H_s(q^{-1}). \tag{2.22}$$

If furthermore the input signal $u(t)$ is persistently exciting[2] then the estimates of the parameter vector $\hat{\theta}_N$ will converge to the true parameter vector θ_0 once the number of available measurements becomes infinite. Notice that identifiability is only guaranteed if infinitely many measurements are available. There are, however, no restrictions on the model structure.
If only the plant is to be identified, $G(q^{-1}) \in \mathcal{G}$,but $\mathcal{S} \notin \mathcal{M}$, i.e.

$$\exists \theta_0 : G(q^{-1}, \theta_0) = G_s(q^{-1}) \text{ but } H(q^{-1}, \theta_0) \neq H_s(q^{-1}), \tag{2.23}$$

$$\hat{G}(q^{-1}, \hat{\theta}_N) \longrightarrow G_s(q^{-1}) \text{ for } N \to \infty, \tag{2.24}$$

if

- open-loop operation ($u(t)$ and $e(t)$ independent).
- $u(t)$ is persistently exciting.
- $G(q^{-1}, \theta)$ and $H(q^{-1}, \theta)$ are parameterized *independently* .

This result is particularly of interest for later analysis of closed-loop identification schemes and is one of the main reasons for transforming closed-loop identification into open-loop equivalents. It guarantees that the true plant can be estimated from the data, but only if infinitely many measurements are available. Furthermore the estimate is unbiased, irrespective of the noise model. In this asymptotic case, it is thus not important whether e.g. an output error or a Box-Jenkins model structure is used. However, when only finite data are available, the situation changes drastically. In this case, a Box-Jenkins structure will probably give a better estimate of the plant's parameters. The reason is that the prediction errors contain a filter, the inverse of the noise model. This filter is adapted automatically during the identification. In an output error structure however, the noise model is fixed and equal to one. Notice, that in an ARX structure the noise model contains the same parameters as the plant model. Therefore the estimates will be biased.

2.4 Closed-loop identification

This section will define the closed-loop identification problem more precisely. Consider the general closed-loop setup as depicted in Figure 2.2. The signal $r(t)$ is an external signal that is chosen to be of sufficient order of excitation. Chapter 3 will further discuss this property and analyze different choices for this excitation. The controller is defined by the polynomials $T(q^{-1})$, $R(q^{-1})$ and $S(q^{-1})$. With respect to the closed-loop setup, the following assumptions are made:

[2] A discussion on this concept is given in chapter 3.

Assumption 2.0
It is assumed that

- The data set$\{r(t), y(t)\}$ is given and either the input $\{u(t)\}$ or the controller is known.
- There is no algebraic loop in the system.
- The closed loop is stable, i.e. the controller stabilizes the plant G_s.

□

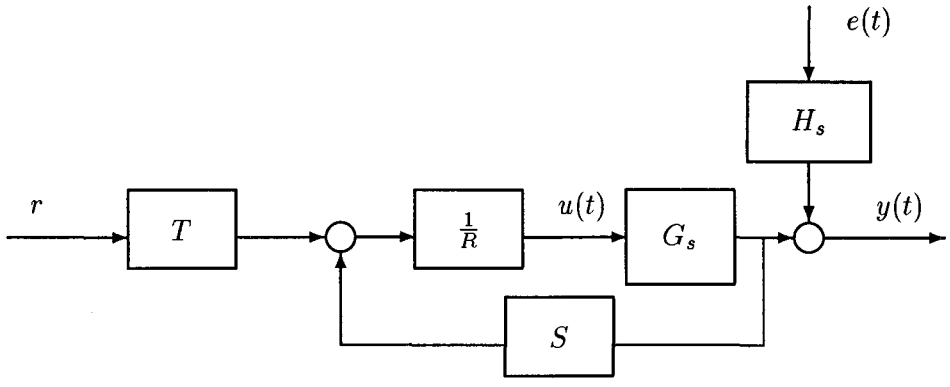

Figure 2.2: General closed-loop setup, under two-parameter control.

If these assumptions are fulfilled the identification experiment can be carried out. The identification method that is used depends on the goal of the identification. Sometimes a consistent estimate of the parameters (including the noise model) is the main goal, but more often the results of an identification experiment will be used to design a new controller. In the latter case not necessarily a consistent estimate of the plant is needed, but the identification must be explicitly tunable to meet the control design requirements. In this report the following requirements, that were adapted from [Van der Klauw (1995)], will be used: *a closed-loop identification method that estimates a model $\hat{G}$ of G_s must have the following properties:*

1. If $G_s \in \mathcal{G}$, but $\mathcal{S} \notin \mathcal{M}$, the estimate $\hat{G}$ must be consistent;
2. The model must be of low order, and hence it only *approximates* the real plant;
3. It should be possible to incorporate control design specifications into the identification procedure, if $\hat{G}(q^{-1}) \neq G_s(q^{-1})$.

A description of "classical" approaches to deal with the closed-loop identification problem can be found in [Söderström and Stoica (1989)]. These methods are referred to as the direct method, the indirect method and the joint input-output method, and should all be seen in the prediction error context. It has been established that under week conditions these methods can consistently identify the true plant, provided that the system is in the set of models that is considered ($\mathcal{S} \in \mathcal{M}$). However, these methods have some drawbacks. The approximation cannot be explicitly tuned and consistency properties are asymptotic, i.e. one needs infinitely

many data to arrive at a consistent estimate of the parameters. The latter is a consequence of the "PEM nature" of these methods. Some examples given below show these properties.

Example 2.3 *Direct identification*
A straightforward way to approach the closed-loop identification problem could be the following. Consider a linear, time invariant discrete time system G_s, that is operated in a closed loop. The setup is depicted in Figure 2.2. Assume that the plant input $u(t)$ and the plant output $y(t)$ are measured. A prediction error method is used to find an estimate of the system. This estimate is known to converge under weak conditions to θ^*, with probability one:

$$\theta^* = \arg\min_{\theta\in\Theta} \frac{1}{2\pi}\int_{-\pi}^{\pi} \Phi_{\varepsilon_f}(\omega)d\omega, \tag{2.25}$$

where Φ_{ε_F} is the spectral density of the filtered prediction error. This expression can be found by applying Parseval's theorem to (lossvn). In an open-loop case, using an output-error model structure with a fixed noise model $H(q^{-1},\theta) = 1$ the resulting estimate θ^* is given by:

$$\theta^* = \arg\min_{\theta\in\Theta} \| [G_s(q^{-1}) - G(q^{-1},\theta)]H_u L \|_2, \tag{2.26}$$

where H_u is a stable spectral factor of Φ_u. Note that the estimate is independent of the noise spectrum. Moreover, the estimate $G(\theta)$ can be "tuned" to make a good approximation in a frequency range emphasized by $H_u L$. On the contrary, in a closed-loop setup the expression for the spectral density of Φ_{ε_F} is

$$\Phi_{\varepsilon_f} = \{| S_s[G_s - G(\theta)] |^2 \Phi_r + \frac{| S_s |^2}{| S(\theta) |^2}\Phi_e\}\frac{| L |^2}{| H(\theta) |^2}. \tag{2.27}$$

Here the actual sensitivity, S_s is equal to $(1 + G_s C)^{-1}$. Note that the estimate is no longer independent of the noise spectrum, and that there does not exist a simple choice of the noise model which could make the Φ_e-dependent term in (2.27) independent of the parameter vector. The consequence is that the estimate $G(\theta)$ will depend on the (unknown) noise spectrum and is not explicitly tunable. □

Example 2.4 *Indirect identification*
Consider a system $G_s(q^{-1})$ that is operating in a closed-loop, as depicted in Figure 2.2. Assuming that the prefilter $T(q^{-1})$ equals one, the closed-loop transfer function can be easily derived:

$$\mathcal{S} : y(t) = \frac{B}{AR + BS}r(t) + \frac{AR}{AR + BS}H_s e(t), \tag{2.28}$$

where $y(t)$ is the closed-loop output and $r(t)$ the reference signal. The noise $e(t)$ enters the loop through H_s at the output of the plant. An indirect identification uses the knowledge of the controller to extract the estimate of the plant from the estimation of the closed loop. The most logical choice for the model structure is thus an ARMAX structure:

$$\mathcal{M} : \bar{A}(q^{-1},\theta)y(t) = \bar{B}(q^{-1},\theta)r(t) + \bar{C}(q^{-1},\theta)\epsilon(t), \tag{2.29}$$

with the interpretation:$\bar{A} = AR + BS, \bar{B} = B$ and $\bar{C} = ARH_s$. But this structure can only give an unbiased estimate of the plant if infinitely many data are available and ARH_s is a polynomial. Furthermore, in the second step the plant must be calculated from:

$$\frac{\hat{B}}{\hat{A}} = \frac{R\bar{B}(q^{-1},\theta)}{\bar{A}(q^{-1},\theta) - S\bar{B}(q^{-1},\theta)}. \tag{2.30}$$

The bias on the estimates now makes that common dynamics in numerator and denominator are not exactly cancelled out. This leads to a high order model and a model reduction step is necessary.

In the chapter 5 the so-called BELS method will be presented. This method takes into account the fact that the parameter estimates in the first step are biased, since an ARX structure is used. Estimation of this bias makes it possible to subtract it from the parameter estimates, thus giving an unbiased identification. □

In practical situations, the data records that one can use to identify the plant are finite. It is known that in this case an instrumental variable approach can give more accurate results. A direct IV method can work also in closed-loop for some systems, but the instruments need to be chosen with care and it is less straightforward than in the open-loop case. An interesting alternative is therefore to transform the closed-loop identification problem into two open-loop ones, where A and B are estimated separately. This is discussed below.

Example 2.5 *Identification of coprime factors*

Consider again the closed-loop setup in Figure 2.2. If the reference signal, the input and the output are known from measurements, they can be used to identify the plant from these data directly. Consider the following equations, describing the closed-loop system:

$$y(t) = \frac{BT}{A_c}r(t) + \frac{ARH_s}{A_c}e(t), \tag{2.31}$$

$$u(t) = \frac{AT}{A_c}r(t) - \frac{ASH_s}{A_c}e(t) \tag{2.32}$$

where A_c is the closed-loop characteristic polynomial. Let the prefilter $T(q^{-1})$ equal one, then

$$y(t) = \frac{B(q^{-1})}{A_c(q^{-1})}r(t) + e_y(t), \tag{2.33}$$

$$u(t) = \frac{A(q^{-1})}{A_c(q^{-1})}r(t) + e_u(t), \tag{2.34}$$

where the noise terms are denoted shortly by $e_y(t)$ and $e_u(t)$. Estimate $B(q^{-1})$, $A(q^{-1})$ and $A_c(q^{-1})$ from (yr) and (ur). Denote the estimates by $\hat{B}(q^{-1})$, $\hat{A}(q^{-1})$, $\hat{A}_{c,y}(q^{-1})$ and $\hat{A}_{c,u}(q^{-1})$. The estimates can now be validated from a comparison of $\hat{A}_{c,y}(q^{-1})$ and $\hat{A}_{c,u}(q^{-1})$ and the calculated closed-loop characteristic polynomial $\hat{A}_{c,calc}$. The latter polynomial is defined as $\hat{A}(q^{-1})R + \hat{B}(q^{-1})S$. This validation test can then be used to determine a suitable model structure.

This method has some drawbacks. As was already established in the section on the prediction error framework, a bias free estimate of the parameters is only possible when infinitely many data are available and the noise model is parameterized independently of the plant model. From the structure of the equations (2.31) and (2.32) though, an ARMAX structure is the most logical choice. Another disadvantage is that no use is made from the fact that the characteristic polynomial A_c is the same in equations (2.33) and (2.34). These problems, however, can be avoided by using a more elaborated scheme. This scheme will be presented in chapter 5 on different methods for closed-loop identification. □

2.5 Alternative identification methods

Recently, alternative methods have been formulated. These methods are mainly directed towards finding a tunable bias expression and consistency for the situation when the system is not in the set of models under consideration ($\mathcal{S} \notin \mathcal{M}$), but the true plant is in the set of plant models ($G_s \in \mathcal{G}$). There are different methods known that can deal with this situation. In this report, the following methods will be examined:

- The two-stage method, see [Van den Hof and Schrama (1993)].
- The dual Youla method, see [Bore-Kuen (1995)].
- The bias elimination least squares method, proposed in [Zheng and Feng (1995)].
- The recursive output error method, see [Landau (1996)].

The characteristics and algorithms of these methods will be discussed in chapter 5. The application to both simulations and a lab-process will give some idea of their performance.

2.6 Identification for control

It was already mentioned that a consistent estimate of the plant is not the only goal. Although a consistent identification can be fruitfully used in model-based controller design, the goal of the latter is clearly to design a controller that meets performance criteria which are based on the controlled process. A discussion on this discrepancy can be found in [Van den Hof and Schrama (1994)]. A matching of the criteria is possible and is proposed in [Åström (1993)]. In this report a new iterative scheme [Holmberg *et al.* (1996)] will be presented and an application of this scheme to a magnetic levitation experiment will be described later. Close to the subject of identification for control is validation for control. This will be discussed at a later stage. A typical controller design validation is given below.

1. Do the identification experiment (in open- or closed-loop setup).
2. Use the estimated model to design a controller, given a certain pole placement of the closed-loop transfer function.
3. The obtained closed-loop poles can now either be calculated from the true plant (in simulations) or estimated from an estimation of the closed-loop directly (in practice).
4. Compare the obtained poles with the designed pole placement.

This procedure gives insight on the resulting closed-loop dynamics, once an estimated model is used for the controller design. It is demonstrated in the example below, that considers both an open-loop and a closed-loop identification.

2.7 Closed-loop versus open-loop identification

In some situations both an open-loop and a closed-loop identification of the unknown system is possible. The example in this section will show that it is very well possible that an identification experiment carried out in a closed-loop setup gives better results than an open-loop

identification experiment. The example system is known as Åströms example. It is a stable plant, with two complex-conjugated poles at $0.75 \pm 0.37i$. The controller was adopted from [Landau (1996)], the noise model from [Van den Hof and Schrama (1993)]. This system will be used as a benchmark example system throughout this report. Its exact properties are given in appendix A.

Example 2.6 *Closed-loop and open-loop identification*
Consider the following plant to be estimated:

$$\mathcal{S}: \begin{cases} y(t) &= G_s(q^{-1})u(t) + H_s e(t), \\ G_s(q^{-1}) &= \frac{q^{-1}+0.5q^{-2}}{1-1.5q^{-1}+0.7q^{-2}}. \end{cases} \tag{2.35}$$

In order to make a fair comparison between the open-loop and the closed-loop identification Landau's recursive output error algorithm will be used for the identification; see [Landau (1996)]. This algorithm is similar for both the uncontrolled and the controlled system. Experiments have been carried out with a constraint on the output, i.e. the experiments were made, such that the signal to noise ratio in the open-loop output as well as in the closed-loop output were equal [3]. In the experiment under consideration, five hundred measurements were made; the noise contribution in the output was approximately equal to twenty-five percent. The following model structure has been chosen:

$$\mathcal{M}: \begin{cases} y(t) &= G(q^{-1},\theta)u(t) + e(t) \\ G(q^{-1},\theta) &= \frac{b_1 q^{-1}+b_2 q^{-2}}{1+a_1 q^{-1}+a_2 q^{-2}}, \end{cases} \tag{2.36}$$

where the parameter vector θ consists of the coefficients a and b. Notice, that the model has an output error structure. Consequenly, the noise model is not estimated. The estimated model was used to construct a controller, such that the resulting closed-loop poles equal pre-specified ones. Thus, for both estimated models a controller was designed, based on a pre-specified pole placement. This validation gives insight in the 'value' of the obtained model for control purposes. The results are given in the figures below, together with the parameter estimates as they evolved in time. □

[3] The signal to noise ratio is here defined at the output as the ratio of the standard deviation in the signal and the standard deviation in the noise.

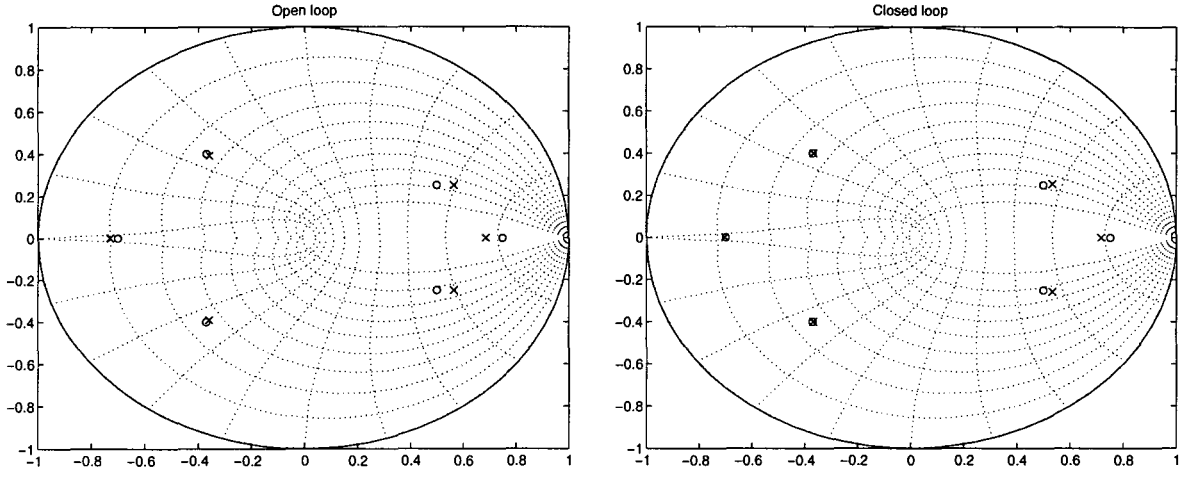

Figure 2.3: Closed-loop from open-loop (a) and closed-loop (b) identification, o: the designed closed-loop poles, x: the obtained closed-loop poles.

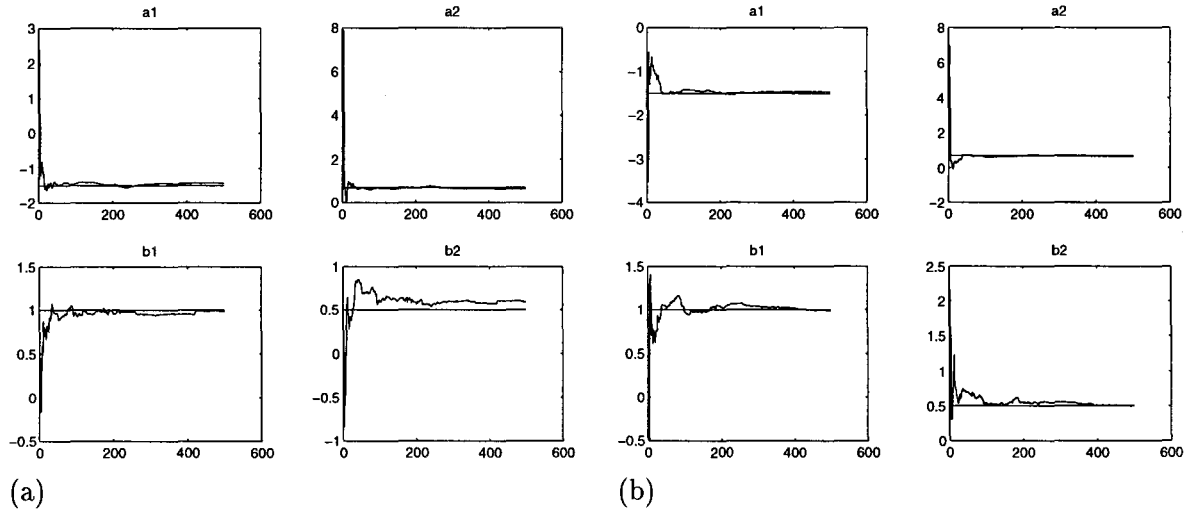

Figure 2.4: Estimates of the parameters during time, in open loop (a) and closed loop (b).

III

Input signals

This chapter will consider input signals. The success of any (parametric or nonparametric) identification depends not only on the identification algorithm that has been used, but also on the excitation of the system. Examples of different input signals are a step function, a white noise, a pseudorandom binary sequence and a periodic excitation. The first section describes some important properties of an input signal. It has been established [Godfrey (1993)], [Schoukens *et al.* (1994)] that multisines can be fruitfully used in an identification experiment. They are introduced in the second section. The third section considers the effect of the input signal on the identified model. This is illustrated with an example, showing the Nyquist plots of an approximate identification with two different input signals.

3.1 Properties of input signals

This section treats the different properties of input signals. The characteristics that will be looked at are the *mean*, *spectral properties*, the *order of persistent excitation* and the *Crest factor*.

Definition 3.1 *Mean of a signal*
Consider a stochastic signal $u(t)$. Its mean or first order moment is defined as:

$$m = \mathrm{E}[u(t)], \tag{3.1}$$

where E denotes the expectation operator. □
For deterministic signals the expectation operator can be changed to the limit of a normalized sum: $\mathrm{E} \rightarrow \lim_{N\rightarrow\infty} \frac{1}{N} \sum_{t=1}^{N}$, assuming that the limit exists. In the analysis of identification algorithms it is sometimes convenient to use expectations instead of finite sums, if the number of data tends to infinity. Stochastic signals for which the finite limit reaches the expectation value with probability one, as $N \rightarrow \infty$, are called *ergodic* . A zero mean of an input signal is of importance, since this is assumed in most model structures. The mean of the measured signals must therefore be removed before the identification.

Definition 3.2 *Power spectrum*
The power spectrum of a stochastic signal $u(t)$ is given by:

$$\Phi_u(k) \equiv u(k)u^*(k), \tag{3.2}$$

where $u(k)$ is the k-th Fourier coefficient. □

A necessary condition for the consistent estimation of a n-th order linear system is that the input signal is persistently exciting of order n. This means that the input signal is rich enough to excite all modes of the unknown system and to make an identification possible. Formally, the order of persistent excitation is defined by:

Definition 3.3 *Order of persistent excitation*
A signal $u(t)$ is said to be persistently exciting of order n if:

(i) the following limit exists:

$$r_u(\tau) = \lim_{N\to\infty} \frac{1}{N} \sum_{t=1}^{N} u(t+\tau)u^{\mathrm{T}}(t) \tag{3.3}$$

(ii)

$$R_u(n) = \begin{pmatrix} r_u(0) & r_u(1) & \dots & r_u(n-1) \\ r_u(-1) & r_u(0) & & \vdots \\ \vdots & & \ddots & \\ r_u(1-n) & \dots & \dots & r_u(0) \end{pmatrix} \tag{3.4}$$

is positive definite.

□

This definition was adapted from [Söderström and Stoica (1989)]. If the signal $u(t)$ is ergodic, then the sum in (3.3) can be replaced by the expectation operator E. Then, the matrix $R_u(n)$ becomes the usual covariance matrix (supposing that $u(t)$ has zero mean).
The concepts defined above give the possibility to construct an input signal that is rich enough to identify all the parameters of a model and can furthermore be tuned with respect to its spectral densities. The question is, however, if a chosen input signal is *efficient*, and how this efficiency can be determined. The Crest factor can be used to measure the density of a signal. This factor is defined as the quotient of the peak value and the root mean square value of the signal. For a continuous time signal, the Crest factor is defined below.

Definition 3.4 *Crest factor*
The Crest factor CF_u of a continuous time signal $u(t)$ is given by

$$CF_u = \frac{l_\infty[u]}{l_2[u]}, \tag{3.5}$$

where l_∞ is the Chebyshev norm of u and l_2 denotes the 2-norm. □

The above definition is valid for continuous time functions $u(t)$. In discrete time, where the signal $u(t)$ is sampled at a certain frequency, the following approximation can be used:

$$CF_u \approx \frac{L_\infty[u(t_n)]}{L_2[u(t_n)]}. \tag{3.6}$$

Here, t_n is used to stress the discrete time nature of the L_p norms. If trigonometric signals are used and the sampling is done at equally spaced time intervals, an upper and a lower bound for the approximation can be computed. See [Guillaume *et al.* (1991)] and appendix B.

3.2 Multisines

Since the multisine will turn out to be of great value in the identification procedure, a definition is given below.

Definition 3.5 *Multisine*
A multisine is the sum of a number of harmonically related sinusoids with programmable amplitudes a_n:

$$u(t) = \sum_{n=1}^{N} a_n \cos(2\pi k_n t/T + \alpha_n), \quad t = iT_s, i = 1, 2, ..., M. \tag{3.7}$$

The phase shift is here denoted by α_n, while the included harmonics are represented by k_n ($k_n \in \mathrm{N}, n = 1, 2, ..., N$ and $0 < k_1 < k_2 < ... < k_N$). The period of the excitation is T, the sampling time is T_s. The number of data that is used is given by M, such that $MT_s = pT$, $p \in \mathrm{N}$. □
In [Schoukens *et al.* (1994)] and [Godfrey (1993)] a number of advantages of multisine input signals are discussed. The most important properties with respect to identification are given below.

3.2.1 Improvement of the signal to noise ratio

The signal to noise ratio can be ameliorated by:

- Minimization of the Crest factor
- Selection of frequency lines
- Time domain averaging

The minimization of the Crest factor will be discussed later. With regard to the selection of the frequency lines, multisines contain only pre-specified frequencies. This knowledge can be used to eliminate all other frequencies in both the input and the output spectrum that do not contribute to the experiment. This advantage is valid essentially for the frequency domain, although the application of a fast Fourier transform and an inverse FFT, putting the non-excitation lines to zero, can ameliorate the results also in the time domain. This procedure can also lead to an improvement of the finite sample behaviour of the identification scheme. It is shown by [Schoukens *et al.* (1994)] that the risk that the identification scheme gets trapped in a local minimum decreases once all non-excitation lines are removed from both the input and the output spectra. Furthermore, the periodic nature of a multisine makes it possible to do a time domain averaging. These procedures do all contribute to a better signal to noise ratio.

3.2.2 Simplify the model validation

The next chapter will explain that a model validation is a necessary step in the identification process. One way to do a validation is a validation in the frequency domain. If periodic excitations are used, it is very simple to obtain a good measurement of the non-parametric transfer function. See e.g. [Guillaume *et al.* (1992)]. The latter article even claims that

an unbiased estimate of the non-parametric transfer function is possible in a closed-loop identification experiment, using the plants input and output. In this report, however, is focused on short data records and therefore no advantage can be taken of nonparametric estimates.

3.2.3 Crest factor minimisation

A more dense input signal leads to a increment of the signal to noise ratio for a given peak value or to a reduced peak value for a given SNR. The latter leads to a reduction of the non-linearities which can be hidden in the studied system. The reduction of the Crest factor can be done in different manners, see e.g. [Guillaume *et al.* (1991)] or [Godfrey (1993)]. The search of the phases is a highly non-linear problem. Schroeder (see e.g. [Godfrey (1993)]) proposed the following (empirical) phase selection:

$$\alpha_n = \alpha_1 - 2\pi \sum_{k=1}^{n-1} (n-k) P_k, \tag{3.8}$$

where P_k is the relative power of the kth component. For a multisine with a flat-amplitude spectrum, (3.8) reduces to:

$$\alpha_n = -\frac{\pi(n-1)n}{N}. \tag{3.9}$$

Here, only input signals with a flat amplitude spectrum will be considered, and Schroeders formula will be used for the optimization of the Crest factor. The phase selection for a multi sine of ten sines is depicted in Figure 3.1, together with the resulting input signal for a flat amplitude spectrum.

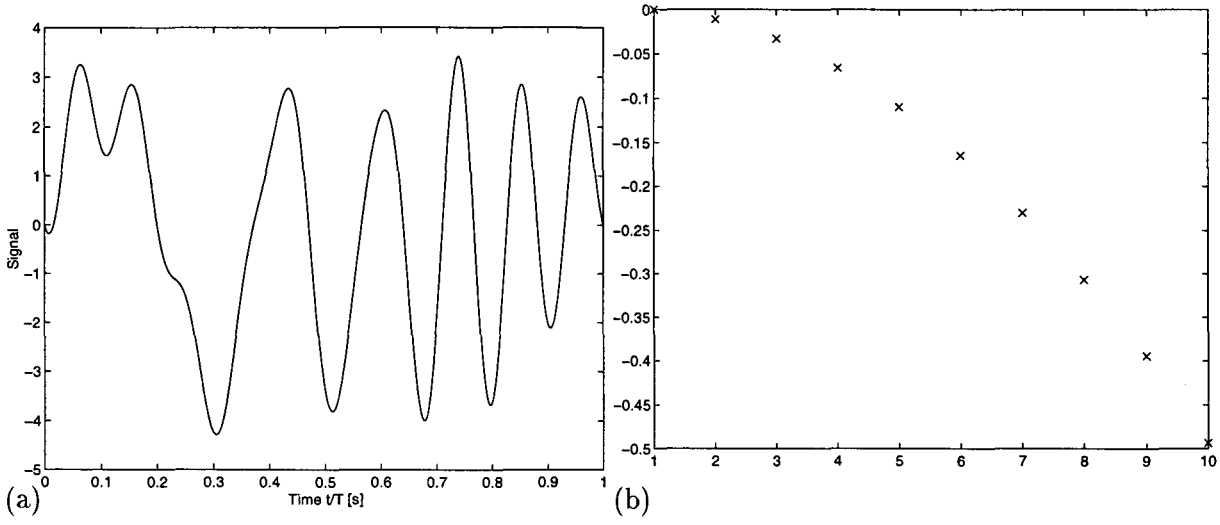

Figure 3.1: Multisine of ten sines: (a) Multisine, (b) Phase selection. The resulting Crest factor is equal to 1.92.

3.2.4 Selection of harmonics

The introduction from this chapter already mentioned that the outcome of an identification experiment not only depends on the identification method that is used, but also on the input signal that is chosen. A multisine input signal can easily be tuned by the a selection of the amplitudes of the different components. The problem is, however, that in order to design an optimal input signal, one needs information on the (unknown) plant. It is therefore not easy to select a proper input signal. But sometimes, some characteristics of the controlled system are already known, from e.g. the Nyquist curve identification as discussed in the next chapter on validation. Especially the frequencies which determine the (controlled) systems behaviour, the frequency range between the crossover frequency and the critical frequency, are important to identify. This gives a first selection of the harmonics to be included in the input signal. A multisine input signal then inserts all input energy into this specific frequency region, that is shown in Figure 4.2.

IV

Validation

4.1 Introduction

It was already mentioned that the objectives of an identification experiment are not always the same. An estimation of the 'true' parameters could be a goal as well as the identification of a model for control purposes. These different objectives demand for different validation methods. In this chapter four different validation procedures are presented and explained. They are gathered in the table below together with their respective goal.

Objective of identification	*Validation Method*
Estimation of 'true' parameters	Statistical test
	Sum of squares test
Determination of model structure	Uncorrelation test
Identification for control	Pole closeness test
	Ziegler-Nicols test

Table 4.1: Methods for validation.

4.2 Statistical test

A straightforward way to do a validation test, is to compare the true parameters that describe the system with the estimated parameters. Especially when a simulated system is used, e.g. for comparison of different identification schemes, the true parameters are known, and Monte-Carlo loops can be carried out in order to determine the statistical characteristics of the estimates: mean and variance. This gives an idea of the performance of the identification scheme and makes it possible to compare different identifications, done with different settings of the estimation algorithm. When the plant to be estimated is unknown, it is not always possible to run a lot of experiments to arrive at a validation. In this case it is better to use one of the methods mentioned below, that give the means for validation after every experiment that is carried out.

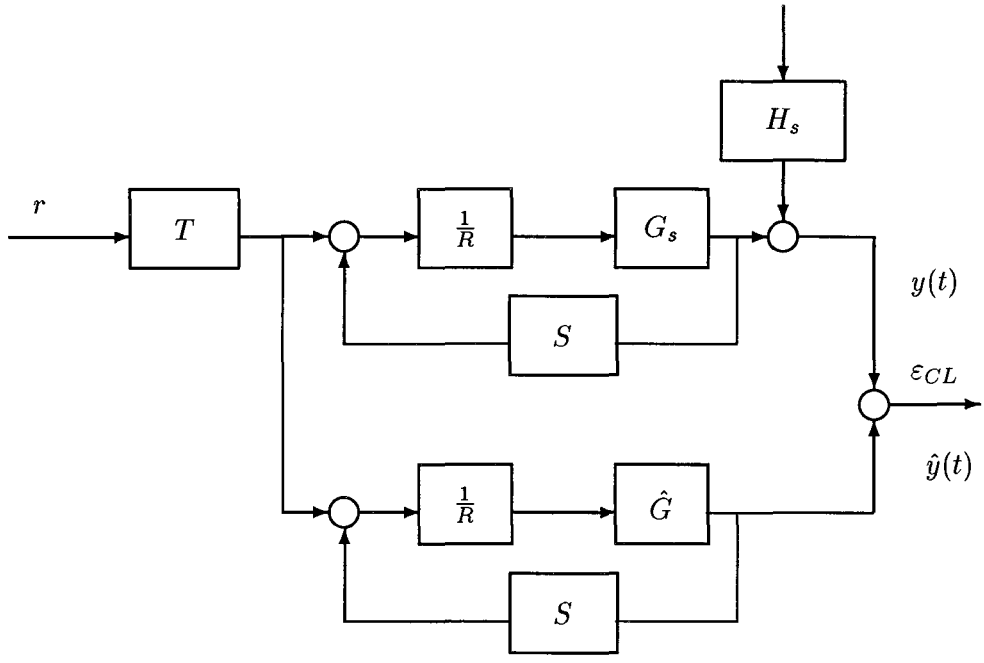

Figure 4.1: Setup for the uncorrelation test

4.3 Uncorrelation test

A method that can test whether all the dynamics of the system are explained by the model is an uncorrelation test. The setup from Figure 4.1 can easily be implemented. The data that are used for this validation can either be the measurements that were used for the identification experiment or new measurements. The uncorrelation between ε_{CL} and $\hat{y}(t)$ shows how well the dynamics of the true plant are incorporated in the estimated model. Note that this test is controller dependent.

4.4 Pole closeness test

A pole closeness test is an easy way to do a model validation. Where a statistical validation can only be performed when a true plant is known and $\mathcal{P} \in \mathcal{G}$, a pole-closeness test can also be performed when an approximate identification has been carried out. The test consists of three steps:

1. Identification of the closed-loop poles, by e.g. a coprime factor identification
2. Calculation of the closed-loop poles from the estimated model and the (known) controller
3. Comparison

In step 1, *obtained* closed-loop poles are estimated (which is an open-loop identification problem), while in step 2, the designed closed-loop poles are computed based on the identified

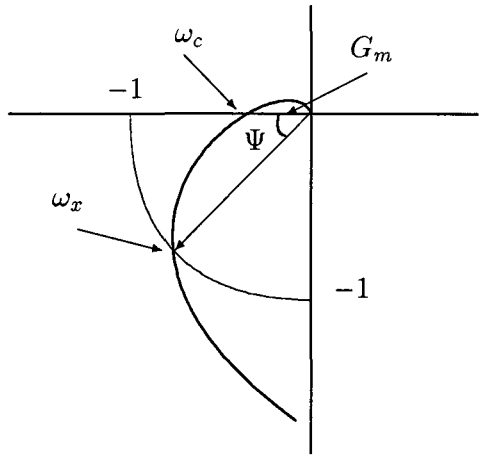

Figure 4.2: Typical Nyquist plot of the open-loop controller system, ω_x is the crossover frequency, ω_c is the critical frequency.

model. The comparison is made with regard to the closeness of dominant (slow) poles.

4.5 Sum of squares test

This time domain test calculates

$$V_N(\theta) = \frac{1}{N}\sum_{t=1}^{N}\left[\varepsilon_f^2(t,\theta)\right], \tag{4.1}$$

where the filter was chosen equal to unity, throughout this report. The value of this loss function shows the quality of the obtained model.

4.6 Frequency domain tests

This validation checks if the frequency domain characteristics of the identified model match the characteristics of the true plant. However, the difficulty here is that only finite data are available. A nonparametric identification of e.g. the Bode curves can therefore not be performed with a high accuracy. But a Ziegler-Nicols test can very well be carried out to obtain an estimate of the Nyquist curve of the open-loop controlled system, i.e. CG ($C = S/R$). A typical Nyquist plot is depicted in Figure 4.2. The gain margin is now defined as the inverse of G_m; the phase margin is defined as Ψ, ω_x is the crossover frequency and ω_c is the critical frequency. If the gain in the controller polynomial S is augmented, the gain margin will become smaller and reach one, when the point -1 is reached by the Nyquist curve. At this point, the system starts to self-oscillate with the frequency ω_c and an estimate of the plant can be made as

$$\hat{G}(\mathrm{e}^{-i\omega_c T_s}) = -\frac{1}{C(\mathrm{e}^{-i\omega_c T_s})}, \tag{4.2}$$

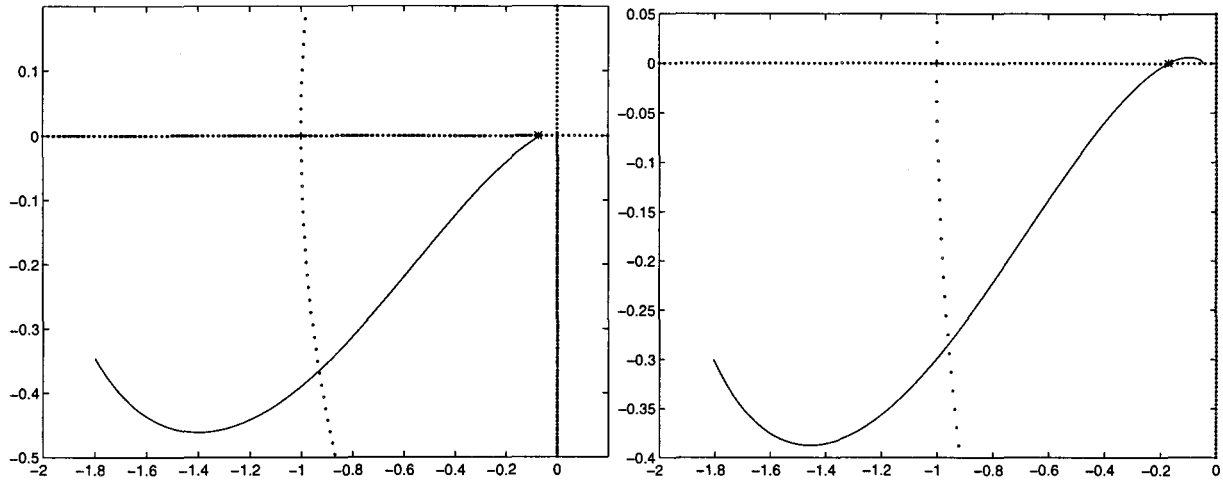

(a) (b)

Figure 4.3: Nyquist plot of the open-loop controlled system; (a) $\alpha = 0$, (b) $\alpha = 0.2$.

since the controller C is known. The frequency ω_c can be estimated from a parametric estimate for under an ARX model structure:

$$\mathcal{M} : model = \frac{1}{1 + a_1 q^{-1} + a_2 q^{-2}}. \tag{4.3}$$

Taking r_1 as one of the roots of the denominator polynomial, the estimate of the crossover frequency is:

$$\omega_c = | \left[\arctan \frac{Im(r_1)}{Re(r_1)} \right] |. \tag{4.4}$$

This estimate can be compared with a parametrically identified model, but for this frequency only! In order to identify more points on the Nyquist curve, a low pass filter $\frac{1-\alpha}{1-\alpha q^{-1}}$, with $1 < \alpha \leq 0$ can be incorporated in the controller. This will rotate the Nyquist curve and consequentially the critical frequency will change for this new situation. The experiment as described above can again be carried out. The figures below show the Nyquist curve of the open-loop controlled system, with $\alpha = 0$ to $\alpha = 0.5$ [1].

α	*Gain margin*	*Critical frequency [rad]*
0.0	13.73	3.14
0.2	5.81	1.21
0.35	2.72	0.73
0.5	1.42	0.44

Table 4.2: Ziegler Nicols identification of the Nyquist curve.

[1] In contrast to the other examples, the system that was used to create this plots was not the system from Åströms example, but a first order plant under RST control.

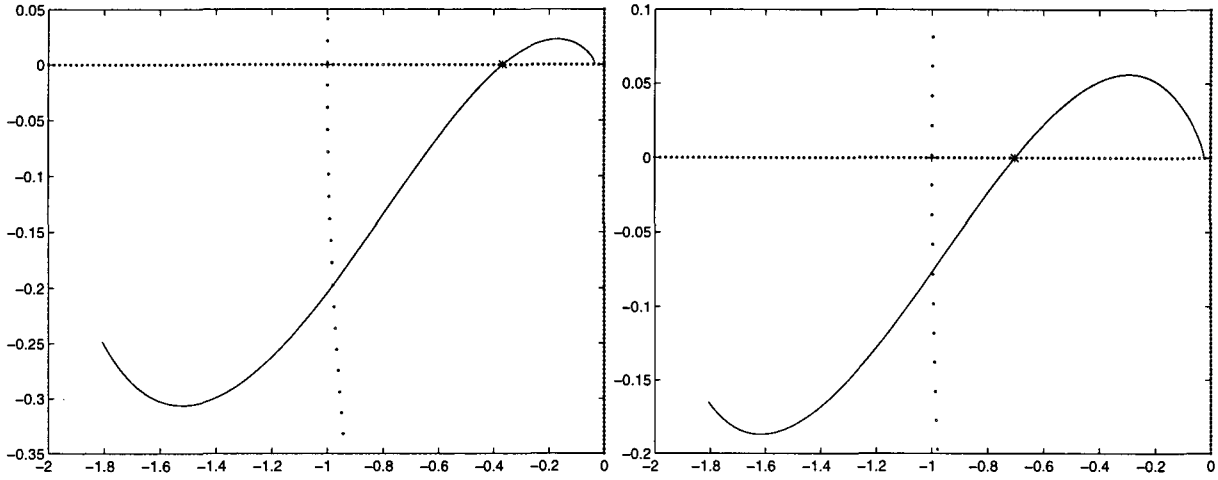

Figure 4.4: Nyquist plot of the open-loop controlled system; (a) $\alpha = 0.35$, (b) $\alpha = 0.5$.

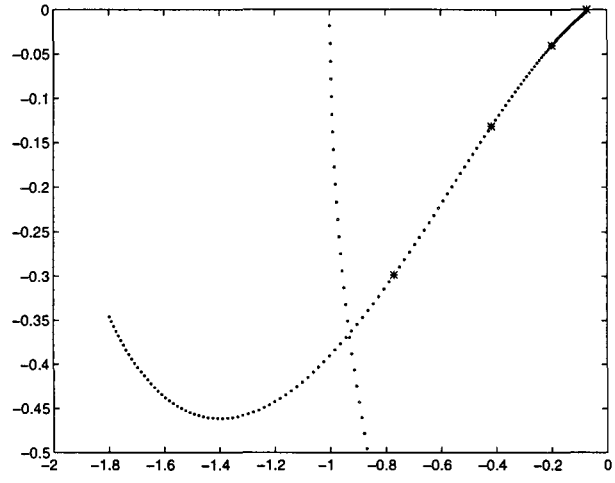

Figure 4.5: Reconstruction of the Nyquist plot of the open-loop controlled process.

A validation in itself for this test consists of the computation of the power spectrum. This spectrum should show one peak at the oscillation frequency. Even when few data are available, the spectrum gives some information on the frequency of oscillation. This validation will be illustrated in chapter 6 for a magnetic levitation experiment.

V

Methods for closed-loop identification

In this chapter different methods for identification in closed-loop will be discussed. The properties of the different methods are clarified by an example. The first section of this chapter is devoted to the identification algorithms, the second section shows the results from an identification experiment. Since the description of the different approaches is short, for more details is referred to the bibliography, especially with regard to convergence properties. At the end of the second section, an iterative identification for control method is included. The last section shows an identification experiment, that was carried out on an example system. An application from these methods to a real life system can be found in chapter 6.

5.1 Algorithms

5.1.1 Two Stage Method

The introductory chapter on identification mentioned that a possible solution for the closed-loop identification problem is a transformation to an open-loop identification problem. This solution is used in the two stage method ([Van den Hof and Schrama (1993)]), although no use is made of the dual Youla parameterization. Assume that the true system is given by:

$$\mathcal{S} : y(t) = G_s(q^{-1})u(t) + H_s(q^{-1})e(t), \tag{5.1}$$

under one-parameter control, where $S(q^{-1})$ and $R(q^{-1})$ are collected in a controller $C = S(q^{-1})/R(q^{-1})$,

$$u(t) = r(t) - Cy(t). \tag{5.2}$$

The closed-loop behaviour can be expressed as:

$$y(t) = G_s u(t) + H_s e(t), \tag{5.3}$$

$$u(t) = \frac{1}{1+G_sC} r(t) - \frac{H_sC}{1+G_sC} e(t). \tag{5.4}$$

Introduction of the sensitivity function $S_s(q^{-1}) = (1+G_sC)^{-1}$ shortens this equation to:

$$\mathcal{S}_1 : u(t) = S_s r(t) + H_s C S_s e(t). \tag{5.5}$$

This is the (open-loop) system that must be identified in the first step of the algorithm. Since the input $u(t)$ is known, the system can be modelled by:

$$\mathcal{M}_1 : u(t) = S(q^{-1}, \beta)r(t) + R(q^{-1}, \gamma)\epsilon_u(t), \tag{5.6}$$

where β is the parameter vector. The parameters are then estimated using a prediction error technique. The estimated parameters are collected in the vectors $\hat{\beta}$ and $\hat{\gamma}$. Note that $S(\beta)$ and $R(\gamma)$ are parameterized independently to obtain an unbiased estimate of the parameters β. This completes the first step of the algorithm. In the second step, the estimate of the sensitivity function is used to identify the plant. Defining $u^r(t) = T(q^{-1})r(t)$, equation (5.3) can be rewritten to

$$\mathcal{S}_2 : y(t) = G_s u^r(t) + H_s(1 + CS_sG_s)e(t), \tag{5.7}$$

Since $u^r(t)$ is not available from measurements, a *reconstruction* of this signal,

$$\hat{u}^r(t) = S_s(q^{-1}, \hat{\beta})r(t), \tag{5.8}$$

should be used in the second step. System $\mathcal{S}_2$ can be modelled by

$$\mathcal{M}_2 : y(t) = G(q^{-1}, \theta)\hat{u}^r r(t) + H(q^{-1}, \eta)\epsilon_y(t). \tag{5.9}$$

Notice that the plant and the noise model are modelled independently, in order to arrive at unbiased estimates for the plant. The parameter estimates are collected in the vectors θ and η.

5.1.2 Dual Youla parameterization

In the two stage method the closed-loop identification problem was transformed to two open-loop problems, estimating not only the plant but also the sensitivity function. In the Chapter 2, an example was given on the identification from the closed-loop data directly, see example 2.4. There, the closed-loop identification problem was reduced to two open-loop problems. It is, however, possible to do the identification by only one open-loop estimation procedure. This approach is based on the dual Youla parameterization and will be explained in this section. For details is referred to [Bore-Kuen (1995)]. In short, the knowledge of the controller is used to find a set of plant models that are stabilized by this controller. It can be shown that all the models in this set can be parameterized with respect to *one* nominal plant model. Since the true plant is stabilized by the controller, it is a member of this set and consequentially, it can be expressed as a function of the nominal plant model. As a result, the identification problem reduces to an identification of one transfer function.
Consider a plant G_s, H_s that is controlled by a RST controller:

$$\mathcal{S} : y(t) = G_s u(t) + H_s e(t). \tag{5.10}$$

Assume that the transfer functions G_s and H_s can be written as coprime factorisations:

$$G_s = \frac{N_s}{D_s}, \tag{5.11}$$

$$H_s = \frac{C_s}{D_s}, \tag{5.12}$$

where N_s, D_s and C_s are polynomials in the backward shift operator. From the experimental setup (Figure 2.2), the characteristic polynomial can be found to be:

$$N_sS + D_sR = U, \tag{5.13}$$

where U is some stable polynomial. From the nature of the true system, it is natural to use an ARMAX model structure:

$$\mathcal{M} : A(q^{-1})y(t) = B(q^{-1})u(t) + C(q^{-1})\epsilon(t), \tag{5.14}$$

where A, B and C are polynomials in backward shift. With regard to this model structure, the set of all possible plants that are stabilized by the controller is given by:

$$G(Q) = \frac{N + QR}{D - QS}, \tag{5.15}$$

$$H(Q, F) = \frac{F}{D - QS}. \tag{5.16}$$

The polynomials N and D are some solution of the Diophantine-Aryabhatta-Bezout (DAB) identity[1]:

$$DR + NS = 1. \tag{5.17}$$

The parameterizing transfer function is Q. The transfer function F defines the numerator of H and as such, the quotient $\frac{F}{D-QS}$ can be seen as a parameterisation of the possible noise models. Let the true plant be given by:

$$G(Q_s) = \frac{D_s + Q_s R}{N_s - Q_s S}, \tag{5.18}$$

$$H(Q_s, F_s) = \frac{F_s}{D_s - Q_s S}. \tag{5.19}$$

Then, the identification of the unknown system reduces to an identification of Q_s and F_s. If the plant only is to be identified, the estimation of Q_s suffices. It can be shown (appendix B) that the parameterized plant can be expressed as:

$$y(t) = (N + Q_s R)r(t) + RF_s e(t), \tag{5.20}$$

$$u(t) = (D - Q_s S)r(t) - SF_s e(t), \tag{5.21}$$

where a prefilter $T = 1$ is assumed. From this, a reduced system can be defined as:

$$\mathcal{S}_r : \beta(t) = Q_s r(t) + F_s e(t), \tag{5.22}$$

$$\beta(t) = Dy(t) - Nu(t). \tag{5.23}$$

Collecting the parameters of Q and C in a parameter vector θ, a model structure for the reduced system is:

$$\mathcal{M}_r : \beta(t) = Q(q^{-1}, \theta)r(t) + F(q^{-1}, \theta)\epsilon(t). \tag{5.24}$$

Since, N and D are known from (5.17), β can be constructed from measurements, and from the resulting reduced plant $Q(q^{-1}, \beta)$ an estimate of the plant can be computed via (5.15). Notice, that the computation of the plant involves the controller. This may lead to a high order plant estimate, making a model reduction step necessary.

[1] The one on the right hand side can be obtained by a normalisation of the controller, see [Bore-Kuen (1995)]

5.1.3 Bias Eliminating Least-squares Method

This subsection gives a description of the BELS (Bias Eliminating Least-squares) Method, see [Zheng and Feng (1995)]. This method estimates the plant indirectly from the closed-loop data. Consider a general closed-loop system under one-parameter control, where $G(q^{-1})$ represents the transfer function of the plant and $C(q^{-1})$ the feedback controller. The input $u(t)$, the output $y(t)$ and the reference $r(t)$ are assumed to be known. The closed loop is defined by

$$y(t) = Gu(t) + e(t), \tag{5.25}$$
$$u(t) = r(t) - Cy(t). \tag{5.26}$$

Both the plant and the controller can be written as a quotient of two coprime factors,

$$\mathcal{S}: \; G(q^{-1}) = q^{-d}\frac{B(q^{-1})}{A(q^{-1})} = q^{-d}\frac{b_1q^{-1} + \ldots + b_{nb}q^{-nb}}{1 + a_1q^{-1} + \ldots + a_{na}q^{-na}}, \quad d \geq 0, \tag{5.27}$$
$$C(q^{-1}) = \frac{Q(q^{-1})}{P(q^{-1})} = \frac{q_0 + q_1q^{-1} + \ldots + q_{nq}q^{-nq}}{1 + p_1q^{-1} + \ldots + p_{np}q^{-np}}, \tag{5.28}$$

where d denotes the number of time delays that are present in the system.

Assumption 5.0
The following assumptions must be made:

- The external signal $r(t)$ is stationary, measurable and persistently exciting of sufficient order.
- The colored disturbance $e(t)$ is a stationary random sequence, independent of $r(t)$.
- The closed loop is asymptotically stable. The polynomials $A(\cdot)$ and $B(\cdot)$, as well as $P(\cdot)$ and $Q(\cdot)$ are coprime.
- The structure parameters, na, nb, np, nq, are given and we know the regulator.
- The order of the polynomial P is greater than or equal to the order of the polynomial A, i.e. $np \geq na$.

□

Notice that both $A(q^{-1})$ and $P(q^{-1})$ are chosen monic. The relationship between the output $y(t)$, the external input $r(t)$ and the disturbance $e(t)$ can be written in ARX notation:

$$\mathcal{A}(q^{-1}) = \mathcal{B}(q^{-1})r(t) + \xi(t), \tag{5.29}$$

where

$$\mathcal{A}(q^{-1}) = A(q^{-1})P(q^{-1}) + q^{-d}B(q^{-1})Q(q^{-1}) \tag{5.30}$$
$$= 1 + \alpha_1q^{-1} + \alpha_2q^{-2} + \ldots + \alpha_{n\alpha}q^{-n\alpha}, \tag{5.31}$$
$$\mathcal{B}(q^{-1}) = q^{-d}B(q^{-1})P(q^{-1}) \tag{5.32}$$
$$= q^{-d}\left(\beta_1q^{-1} + \beta_2q^{-2} + \ldots + \beta_{n\beta}q^{-n\beta}\right). \tag{5.33}$$

In this equations, $n\alpha = \deg[\mathcal{A}(q^{-1})] = \max[na + np, nb + nq + d]$ and $n\beta = np + nb$, while $\deg[\mathcal{B}(q^{-1})] = nb + np + d$. Further, since $\mathcal{A}$ is chosen monic and A, P are monic it is implicitly assumed that $d \geq 0$. Further, the disturbance in closed loop can be written as:

$$\xi(t) = A(q^{-1})P(q^{-1})e(t). \tag{5.34}$$

Introduce the closed-loop parameter vector ϑ,

$$\vartheta = [\alpha_1, \alpha_2, \ldots, \alpha_{n\alpha}, \beta_1, \ldots, \beta_{n\beta}]^{\mathrm{T}}, \tag{5.35}$$

with length $n\alpha + n\beta$. Write the closed-loop equation (5.29) as:

$$y(t) = \psi(\mathbf{t})^{\mathrm{T}}\vartheta + \xi(t), \tag{5.36}$$

where

$$\psi(t) = [-y(t-1)\ldots - y(t-n\alpha)\, r(t-k-1)\ldots r(t-k-n\beta)]^{\mathrm{T}}. \tag{5.37}$$

Next, create a matrix Ψ containing all observations,

$$\Psi^{\mathrm{T}} = [\psi(1), ..., \psi(N)], \tag{5.38}$$

a vector $\mathbf{y}$ of all the measurements and a vector ξ of errors. Then the following holds:

$$\mathbf{y} = \Psi\vartheta + \xi. \tag{5.39}$$

A least-squares estimate of ϑ is given by:

$$\hat{\vartheta}_{\mathbf{LS}}(N) = \Psi^{\dagger}\mathbf{y}. \tag{5.40}$$

$\Psi^{\dagger}$ denotes the general inverse of Ψ, $\Psi^{\dagger} = (\Psi^{\mathrm{T}}\Psi)^{-1}\Psi^{\mathrm{T}}$, which is assumed to exist, due to the first assumption above. It can be shown that the least-squares estimate $\hat{\vartheta}_{\mathbf{LS}}$ is biased with respect to the true parameter vector ϑ,

$$\hat{\vartheta}_{\mathbf{LS}} = \vartheta + \Delta\vartheta(N), \tag{5.41}$$

where

$$\Delta\vartheta(N) = \Psi^{\dagger}\xi = \hat{\mathbf{R}}_{\psi\psi}^{-1}(N)\hat{\mathbf{R}}_{\psi\xi}(N), \tag{5.42}$$

$$\hat{\mathbf{R}}_{\psi\psi}(N) = \frac{1}{N}\sum_{t=1}^{N}\psi(t)\psi(t)^{\mathrm{T}}, \tag{5.43}$$

$$\hat{\mathbf{R}}_{\psi\xi}(N) = \frac{1}{N}\sum_{t=1}^{N}\psi(t)\xi(t) = \begin{bmatrix} \hat{\mathbf{R}}_{\mathbf{y}\xi}(N) \\ \hat{\mathbf{R}}_{\mathbf{r}\xi}(N) \end{bmatrix}. \tag{5.44}$$

The bias $\Delta\vartheta(N)$ cannot be computed. The reason is that $\xi(t)$ is not measurable. Therefore $\hat{\mathbf{R}}_{\psi\xi}(N)$ cannot be computed. The idea is to replace $\hat{\mathbf{R}}_{\psi\xi}(N)$ with an expression $\hat{\hat{\mathbf{R}}}_{\psi\xi}(N)$ that can be calculated and is a good approximation for large N. Introduce

$$\mathbf{R}_{\psi\psi} = \mathrm{E}\left[\psi(t)\psi(t)^{\mathrm{T}}\right], \tag{5.45}$$

$$\mathbf{R}_{\psi\xi} = \mathrm{E}[\psi(t)\xi(t)] = \begin{bmatrix} \mathbf{R}_{\mathbf{y}\xi} \\ \mathbf{R}_{\mathbf{r}\xi} \end{bmatrix} = \begin{bmatrix} \mathbf{R}_{\mathbf{y}\xi} \\ \mathbf{0} \end{bmatrix} = \Xi\mathbf{R}_{\mathbf{y}\xi}, \tag{5.46}$$

then it holds that

$$\lim_{N\to\infty} \hat{\mathbf{R}}_{\psi\psi}(N) = \mathbf{R}_{\psi\psi}, \tag{5.47}$$

$$\lim_{N\to\infty} \hat{\mathbf{R}}_{\psi\xi}(N) = \mathbf{R}_{\psi\xi}. \tag{5.48}$$

In (5.46) we use that r and ξ are uncorrelated and introduce for convenience the projection matrix $\Xi = [\mathbf{I}_{n\alpha} \ \mathbf{0}_{n\alpha\times n\beta}]^{\mathrm{T}}$. It can be shown below, that $\hat{\mathbf{R}}_{\mathbf{y}\xi}(N)$ actually can be approximated for large N when knowledge of the controller is taken into account. Therefore it makes sense, for a long enough data record, to choose

$$\hat{\hat{\mathbf{R}}}_{\psi\xi}(N) = \Xi\hat{\hat{\mathbf{R}}}_{\mathbf{y}\xi}(N), \tag{5.49}$$

where $\hat{\hat{\mathbf{R}}}_{\psi\xi}(N)$ is an approximation for $\hat{\mathbf{R}}_{\psi\xi}(N)$. Notice, though, that $\hat{\hat{\mathbf{R}}}_{\psi\xi}(N) \neq \hat{\mathbf{R}}_{\psi\xi}(N)$ for small N. The bias is, thus, estimated as

$$\Delta\vartheta(N) = \hat{\mathbf{R}}_{\psi\psi}(N)^{-1}\hat{\hat{\mathbf{R}}}_{\psi\xi}(N), \tag{5.50}$$

and the bias-eliminated estimate is:

$$\hat{\vartheta}_{BELS} = \hat{\vartheta}_{LS} - \Delta\vartheta(N). \tag{5.51}$$

The closed-loop parameter vector ϑ can be related to the open-loop parameter vector θ by,

$$\vartheta = \mathbf{M}\theta + \rho, \tag{5.52}$$

where $\rho = [p_1, ...p_{np}; 0, ..., 0]^{\mathrm{T}}$ with length $na + nb$. The size of the matrix $\mathbf{M}$ is equal to $(n\alpha + n\beta) \times (na + nb)$ and can be expressed as

$$\mathbf{M} = \begin{bmatrix} \mathbf{P_1} & \mathbf{Q} \\ \mathbf{0} & \mathbf{P_2} \end{bmatrix}, \tag{5.53}$$

where the matrices $\mathbf{P_1}$ and $\mathbf{P_2}$ are Sylvester matrices expanded by the vector $[1, p_1 \ldots p_{np}]^{\mathrm{T}}$. Their sizes are $n\alpha \times na$, $n\beta \times nb$ respectively. The matrix $\mathbf{Q}$ consists of d rows of zeros above a Sylvester matrix expanded by the vector $[q_0 \ldots q_{nq}]^{\mathrm{T}}$, with size $(n\alpha - d) \times nb$. Therefore the matrix $\mathbf{Q}$ has size $n\alpha \times nb$.
Following to proposition 1 of [Zheng and Feng (1995)] a full column rank matrix $\mathbf{H}$ of size $(n\alpha + n\beta) \times (n\alpha + n\beta - na - nb)$ is defined, such that

$$\mathbf{H}^{\mathrm{T}}\mathbf{M} = 0. \tag{5.54}$$

The columns of $\mathbf{H}$ span the null space of the matrix $\mathbf{M}$. Multiplication of (5.52) by $\mathbf{H}^{\mathrm{T}}$ yields:

$$\mathbf{H}^{\mathrm{T}}\vartheta = \mathbf{H}^{\mathrm{T}}\rho. \tag{5.55}$$

For large N it holds that $\Delta\vartheta(N) = \hat{\vartheta}_{LS} - \vartheta$. Multiply from the left by $\mathbf{H}^{\mathrm{T}}$ to get

$$\left[\mathbf{H}^{\mathrm{T}}\hat{\mathbf{R}}_{\psi\psi}^{-1}(N)\Xi\right]\hat{\hat{\mathbf{R}}}_{\mathbf{y}\xi}(N) = \mathbf{H}^{\mathrm{T}}\left[\hat{\vartheta}_{\mathbf{LS}}(N) - \rho\right]. \tag{5.56}$$

In this last equation, the number of unknowns is $n\alpha$, while the number of equations is $n\alpha + n\beta - na - nb$. In order to have a unique solution, it is required that:

$$n\alpha = n\alpha + n\beta - na - nb \tag{5.57}$$

$$\Rightarrow np = na, \tag{5.58}$$

which corresponds to the fifth assumption above. If $np > na$, there are more equations than variables and there is not necessarily any solution, but approximations, e.g. least-squares approximations, can be found. The overall result is:

$$\hat{\vartheta}_{BELS} = \hat{\vartheta}_{LS} + \hat{\mathbf{R}}_{\psi\psi}^{-1}(N)\Xi\hat{\mathbf{R}}_{y\xi}(N). \tag{5.59}$$

5.1.4 Recursive Output Error

This section outlines briefly the character and some properties of a recursive identification scheme. Within this scheme an output error model structure is employed, fixing the noise model to one. The system is assumed to be operated under a two-parameter control scheme. The complete algorithm for a recursive identification will be given, for both unfiltered data and filtered data. The latter algorithm has different stability and convergence properties. These properties are discussed at the end of this subsection. A more complete treatment of this method can be found in [Landau (1996)]. In an output error structure, the model is given by

$$\mathcal{M} : y(t) = G(q^{-1})u(t) + \epsilon(t) \tag{5.60}$$

where the plant transfer operator can be written as the ratio of two polynomials $B(q^{-1})$ and $A(q^{-1})$

$$G(q^{-1}) = \frac{B(q^{-1})}{A(q^{-1})} = q^{-d}\frac{b_1\, q^{-1} + ... + b_{nb}q^{-nb}}{1 + a_1\, q^{-1} + ... + a_{na}q^{-na}}. \tag{5.61}$$

In the latter equation, d denotes the time delay. The parameter vector θ consists of the coefficients of both polynomials: $\theta = [a_1, ..., a_{na}, b_1, ..., b_{nb}]^T$. Now introduce $B^*(q^{-1}) = qB(q^{-1})$ and $A^*(q^{-1})$ analogously, then the deterministic output of the closed loop is given by

$$y(t+1) = -A^*(q^{-1})y(t) + B^*(q^{-1})u(t-d), \tag{5.62}$$

where $r(t)$ is the reference signal, $u(t)$ is the plant input and $y(t)$ is the plant output. Collecting the parameters of the polynomials $\hat{A}$ and $\hat{B}$ in a parameter vector θ and the observations in a vector $\psi = [-\hat{y}(t), ..., -\hat{y}(t-na+1)\hat{u}(t-d), ..., \hat{u}(t-nb+1-d)]^{\mathrm{T}}$, where $\hat{y}(t)$ and $\hat{u}(t)$ are defined in (5.65) and (5.71) respectively. The *a priori* output is given by

$$\hat{y}^\circ(t+1) = -\hat{A}^*(t)\hat{y}(t) + \hat{B}^*(t)\hat{u}(t-d). \tag{5.63}$$

$$= \hat{\theta}^{\mathrm{T}}(t)\hat{\psi}(t). \tag{5.64}$$

The hats denote the estimate of the property under consideration. The *a posteriori* output is

$$\hat{y}(t+1) = -\hat{A}^*(t+1)\hat{y}(t) + \hat{B}^*(t+1)\hat{u}(t-d). \tag{5.65}$$

From these predictors both the *a priori* error,

$$\varepsilon^\circ(t+1) = y(t+1) - \hat{y}^\circ(t+1), \tag{5.66}$$

as the *a posteriori* error,

$$\varepsilon(t+1) = y(t+1) - \hat{y}(t+1), \tag{5.67}$$

can be defined. Using equations (5.64) and (5.66), the *a priori* error equation can be rewritten to

$$\begin{aligned} \varepsilon^{\circ}(t+1) &= -A^*(t)y(t) + \hat{A}^*(t)y(t) - \frac{B^*(t)q^{-d}S}{R}y(t) \\ &+ \hat{B}^*(t)q^{-d}\frac{S}{R}\hat{y}(t) + \left(B^* - \hat{B}^*\right)q^{-d}\frac{T}{R}r(t). \end{aligned} \tag{5.68}$$

Addition and subtraction of $\left(A^* + \frac{B^*q^{-d}S}{R}\right)\hat{y}(t)$ gives,

$$\begin{aligned} \varepsilon^{\circ}(t+1) &= -\left[A^* - \hat{A}^*(t)\right]\hat{y}(t) + \left[B^* - \hat{B}^*\right]\hat{u}(t-d) \\ &- \left(A^* + \frac{B^*q^{-d}S}{R}\right)\varepsilon(t), \end{aligned} \tag{5.69}$$

$$= \left[\theta - \hat{\theta}(t)\right]^T\psi(t) - \left(A^* + \frac{B^*q^{-d}S}{R}\right)\varepsilon(t), \tag{5.70}$$

where

$$\hat{u}(t-d) = q^{-d}\left[-\frac{S}{R}\hat{y}(t) + \frac{T}{R}r(t)\right]. \tag{5.71}$$

Using this notation, the *a posteriori* error equation can be written as

$$\varepsilon(t+1) = \left[\theta - \hat{\theta}(t+1)\right]^T\psi(t) - \left[A^* + \frac{B^*q^{-d}S}{R}\varepsilon(t)\right], \tag{5.72}$$

$$= \frac{R}{A_c}\left[\theta - \hat{\theta}(t+1)\right]^T\psi(t). \tag{5.73}$$

The polynomial A_c denotes the closed-loop characteristic polynomial:

$$A_c = AR + q^{-d}BS. \tag{5.74}$$

The parameters estimation algorithm is given by

$$\begin{aligned} \hat{y}^{\circ}(t+1) &= \hat{\theta}^T(t)\psi(t) \\ \varepsilon^{\circ}(t+1) &= y(t+1) - \hat{y}^{\circ}(t+1) \\ \varepsilon(t+1) &= \frac{\varepsilon^{\circ}(t+1)}{1 + \psi^T(t)\mathbf{F}(t)\psi(t)} \\ \mathbf{F}^{-1}(t+1) &= \lambda_1\mathbf{F}^{-1}(t) + \lambda_2\psi(t)\psi^T(t) \\ \hat{\theta}(t+1) &= \hat{\theta}(t) + \mathbf{F}(t)\psi(t)\varepsilon(t+1) \end{aligned}$$

Algorithm: 5.0

The parameters λ_1 and λ_2 should be chosen as

$$0 < \lambda_1 \leq 1 \qquad 0 \leq \lambda_2 < 2. \tag{5.75}$$

The parameter λ_2 can usually be taken equal to one. Then, λ_1 acts as a forgetting factor for the algorithm. The calculation of $\mathbf{F}(t+1)$ can be done by the matrix inversion lemma[2];

$$\mathbf{F}(t) = \frac{1}{\lambda_1}\left[\mathbf{F}(t) - \frac{\mathbf{F}(t)\psi(t)\psi^T(t)\mathbf{F}(t)}{\frac{\lambda_1}{\lambda_2} + \psi^T(t)\mathbf{F}(t)\psi(t)}\right]. \tag{5.76}$$

Stability and convergence

The recursive parameter estimation algorithm is assures that:

$$\lim_{t\to\infty} \varepsilon(t+1) = 0 \tag{5.77}$$

$$\lim_{t\to\infty} \varepsilon^\circ(t+1) = 0 \tag{5.78}$$

$$\|\psi(t)\| < c, \quad 0 < \quad c \quad < \infty \quad \forall t \tag{5.79}$$

for all initial conditions $\hat{\theta}(0), \varepsilon^\circ(0), \psi(0)$, if

$$P(q^{-1}) = \frac{R(q^{-1})}{A_c} - \frac{\lambda}{2}, \quad 2 > \lambda \geq \sup \lambda_2(t) \tag{5.80}$$

is a strictly positive real transfer function. Under some extra assumptions, this condition also implies:

$$\text{Prob}\left\{\lim_{t\to\infty} \hat{\theta}(t) = \theta_0\right\} = 1. \tag{5.81}$$

Proofs for both statements can be found in [Landau (1996)].
The condition on P is restrictful since it outrules the use of a controller with integral action (R(0)=0 ¿ P(0)¡0 not SPR). An ad hoc modification of the algorithm is to filter the regression vector as

$$\psi_f(t) = \frac{R}{\hat{A}_c}\psi(t), \tag{5.82}$$

where $\hat{A}_c$ denotes the estimated characteristic polynomial at time t, the parameter estimation algorithm can be applied on filtered data. This filtering has some advantages, with respect to the stability and convergence of the algorithm.

5.1.5 RθR-scheme

Section 2.6 already mentioned that a good estimate of the parameters is not necessarily one that reconstructs the true system. Instead, the identified model must be such that a control design can be based on it. After the implementation of a new controller, a new identification experiment can be performed, giving an iterative scheme of identification and controller design. In literature different approaches can be found. A discussion is given in e.g. [Schrama (1992)]. One of the key issues is to make control and identification mutually supportive, so that something can be said about the convergence of iterations. Another issue

[2] see appendix B

concerns the tendency to consider the variance modeling errors only, assuming that the true system belongs to the model set. But a large model set must be taken into account to enable asymptotic convergence results. From a practical point of view this is too stringent a requirement; see also section 2.3. The method described below relaxes the model set completeness and introduces an adequate performance index. The entry point is a sequential use of the standard least-squares optimization on the system error equation for the purpose of controller design and plant identification. First, a problem definition will be given, from which a control performance criterion will be deduced. Then, a suboptimal solution to the minimization problem will be given: the $R\theta R$-scheme.

Problem definition

Let the true system be

$$\mathcal{S} : A_s(q^{-1})y(t) = B_s(q^{-1})u(t) + e(t) \tag{5.83}$$

under two-parameter control:

$$R(u(t) = -Sy(t) + Tr(t). \tag{5.84}$$

The controller design is based on the equation error model structure

$$\mathcal{M} : Ay(t) = Bu(t) + \varepsilon(t). \tag{5.85}$$

The characteristic polynomial of the closed-loop *model* is

$$A_m = AR + BS, \tag{5.86}$$

while the *actual* closed-loop characteristic polynomial is

$$A_c = A_sR + B_sS. \tag{5.87}$$

The output of the closed loop is

$$y(t) = \frac{BT}{A_m}r(t) + \frac{R}{A_m}\varepsilon(t) \tag{5.88}$$

Introduce the desired response as

$$y_d(t) = \frac{BT}{A_m}r(t), \tag{5.89}$$

then the control performance error can be defined as

$$e_{cp} = y - y_d = \frac{R}{A_m}\varepsilon = \frac{R}{A_m}(Ay - Bu)\,.. \tag{5.90}$$

Introduce a control performance criterion as:

$$J = \mathrm{E}e_{cp}^2 = \mathrm{E}\left\{\lim_{N\to\infty}\frac{1}{N}\sum_{k=1}^{N}e_{cp}^2(k)\right\}. \tag{5.91}$$

From N samples, the criterion can be estimated to be

$$\hat{J} = \frac{1}{N}\sum + k = 1^N e_{cp}^2(k). \tag{5.92}$$

If the poleplacement is chosen, the polynomial A_m is fixed.
The controller polynomial R can be written as a function of A and B. The solution to the pole placement equation can be parameterized by a polynomial Q, [3] making R a function of Q, A and B. Collecting the coefficients of A and B in a parameter vector θ, the optimization criterion is

$$\min_{\theta,Q} J(R(Q,\theta),\theta), \tag{5.93}$$

where θ and Q are members of some specified reduced order space. The optimization is highly nonlinear, but can be solved by replacing the nonlinear problem by a sequence of linear least-squares problems.

The pole placement equation The pole placement equation has infinitely many solutions, that can be parameterized by a polynomial Q:

$$R = R_1 - QB, \tag{5.94}$$
$$S = S_1 + QA, \tag{5.95}$$

where R_1 and S_1 are one particular solution. Defining

$$\varepsilon_B = \frac{B}{A_m}\varepsilon \tag{5.96}$$
$$\varepsilon_{R_1} = \frac{R_1}{A_m}\varepsilon, \tag{5.97}$$

the control performance error (5.90) is linear in Q

$$e_{cp} = \varepsilon_{R_1} - Q\varepsilon_B. \tag{5.98}$$

As a result $J(Q)$ can be minimized by the least-squares method analytically.

Model estimation Both the input and the output can be filtered over $\frac{R}{A_m}$; let

$$u_F = \frac{R}{A_m}u, \tag{5.99}$$
$$y_F = \frac{R}{A_m}y. \tag{5.100}$$

The control performance error (5.90) can then be written as

$$e_{cp} = Ay_F - Bu_F, \tag{5.101}$$

so that $J(\theta)$ is linear in the parameter vector and can minimized analytically by a least-squares method as well.

[3] The approach here is similar to the parameterization in the dual Youla method. But instead of a parameterization of the plant models is chosen for a parameterization of all controllers that stabilize the plant and that maintain the same A_m.

Optimization procedure Let the initial model be summarized in the parameter vector θ_1. This vector is e.g. a result of an open-loop identification or derived from a physical model. A controller based on this model is implemented and a closed-loop excitation of the system is performed. The sampled data from the experiment are used in each of the minimization steps below:

$$\begin{aligned} Q_1 &= \arg\min_Q \hat{J}(R(Q,\theta_1),\theta_1) \\ \hat{\theta} &= \arg\min_\theta \hat{J}(R(Q_1,\theta_1),\theta) \\ \hat{Q} &= \arg\min_Q \hat{J}(R(Q,\hat{\theta}),\hat{\theta}) \end{aligned}$$

Notice that each step is a linear least-squares problem. In the first step an improvement of the R polynomial is calculated. This is a necessary step that prevents disturbance effects from influencing the parameter estimation in the second step. A possible bias in the data will be "modelled" in R, and not in A. Integral action will then automatically be introduced in the controller. From the new model, R must be computed again in the third step, since R is a function of the model and Q.

5.2 Application to an example system

This section will use the system defined by Åström / Van den Hof[4] as a benchmark example. In order to make a fair comparison between the different methods that were examined in this chapter, different validation methods will be applied to the obtained estimates. Several Monte Carlo loops of the identification procedure have been performed in order to arrive at a statistical validation. The orders of the plant were assumed to be known; the signal to noise ration in the output was approximately 10%. The results from the dual Youla method have been left out, because of the high order estimates this method results in. An overview of the obtained parameter estimates (mean and standard deviation) is given in Table 5.1.
The RθR method has not been evaluated statistically. Since several iterations should be made each experiment, it is hard to judge which iteration should be used for this evaluation. However, after five iterations the control performance error doesn't decrease anymore. The model that was obtained by then has been included in Table 5.1 Furthermore, the objective of the RθR method is not the reconstruction of the 'real' plant, but the control performance. Therefore five iterations have been carried out, to get an idea of this property. The results are depicted in Figure 5.1. The model structure was of second order. The parametrizing Q polynomial had one parameter. Consequently a third order controller has been designed. The designed pole placement was the same as the pole placement that was used for the validation tests below. In the sum of squares and the correlation test, the system (i.e. the estimated model after five iterations plus the corresponding controller) have been used. Since the controller changes with the iterations, the RθR Method has not been included in the test on the frequency domain properties of the open-loop controlled system. The outcome of the pole-closeness test is trivial, since the model is designed such that the closed-loop poles match the designed ones.
The pole closeness test was performed with designed poles spread out in the complex plane. The circles denote the obtained poles, the crosses denote the designed poles.

[4]The plant was adapted from [Åström (1993)], the noise model from [Van den Hof and Schrama (1993)].

	a_1	a_2	b_1	b_2
True plant	-1.5	0.7	1.0	0.5
Two Stage	-1.47 ± 0.06	0.65 ± 0.09	1.00 ± 0.02	0.5 ± 0.1
BELS	-1.5 ± 0.4	0.7 ± 1	1.00 ± 0.05	0.5 ± 0.4
Rec. Output Error	-1.50 ± 0.01	0.70 ± 0.01	1.01 ± 0.01	0.49 ± 0.03
RθR Method	-1.53	0.64	0.83	0.40

Table 5.1: Estimated parameters their standard deviation from different methods.

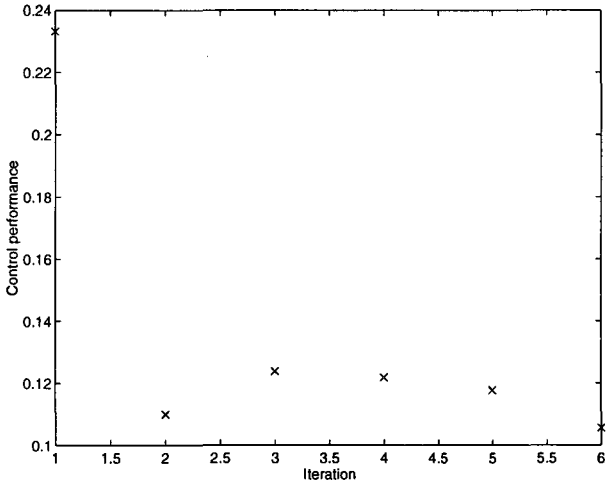

Iteration	Control performance criterion
Initial	0.2332
1	0.1100
2	0.1238
3	0.1218
4	0.1177
5	0.1056

Figure 5.1: Developement of the control performance error for the RθR Method.

	Correlation factor	Sum of squares
Two Stage	0.006	0.01
BELS	0.3	0.02
Rec. Output Error	0.001	0.01
Dual Youla	0.09	0.02
RθR	0.002	0.01

Table 5.2: Correlation factors and sum of squares test (from one experiment).

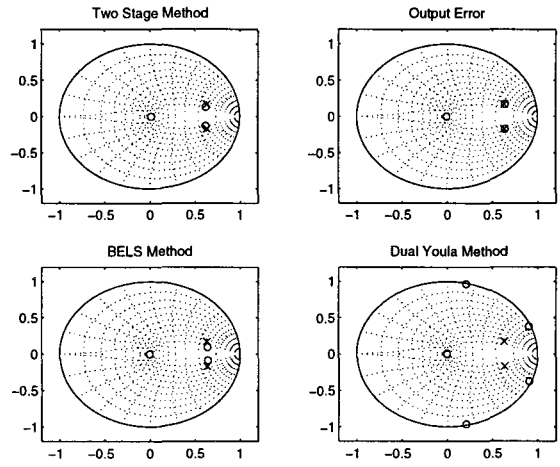

Figure 5.2: Result from the pole closeness test.

	Gain Margin	ω_c	Phase Margin	ω_x
True plant	3.0204	3.1416	50.4885	1.0540
Two Stage	3.0194	3.1416	50.5809	1.0544
BELS	3.1880	3.1416	43.1642	1.0782
Rec. Output Error	3.0940	3.1416	50.1045	1.0602
Dual Youla	2.8698	3.1416	46.6480	1.1323

Table 5.3: Frequency domain properties of the open-loop controlled system.

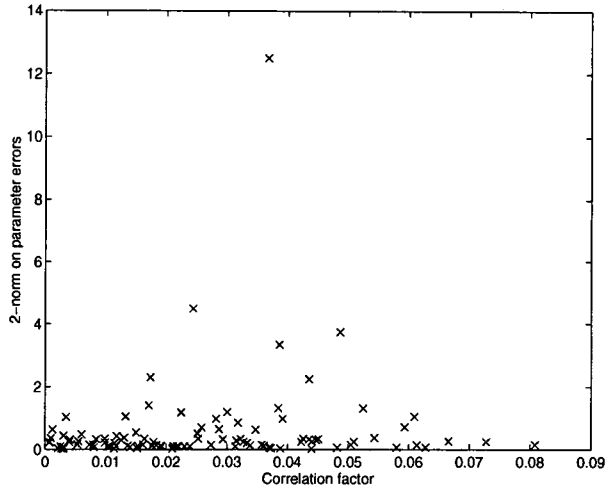

Figure 5.3: Influence of correlation on estimates for the BELS Method.

5.3 Discussion

This section intends to give a discussion on the identification methods that were reviewed above. These methods all differ in approach, they work with different model structures and batch algorithms as well as recursive and iterative algorithms. Furthermore, they include different possibilities for filtering the data and the ability to emphasize certain parts of the frequency domain. It is therefore difficult to make a comparison of these methods.

A possible solution to this problem is the use of validation methods. These methods allow a comparison with respect to a certain objective. The example above clearly shows that a "good" estimate in one respect does not necessarily mean a good estimate in another. Notice that all validation tests were performed with the *same* data record.

Consequently a definite answer to the question on how the identification should be performed can not be given, leaving identification to be more of an art than a method.

However, some remarks on the results above can be made. In Table 5.1 the bias eliminating least squares method shows quite large standard deviations on the estimates of the a_2 and b_2 parameters. This is due to the assumption that the noise is uncorrelated with the input signal. However, in the example, a white noise input signal has been used. Since the data records are short, a correlation between those signals can occur. As a result, the estimate of the correlation matrices fails and so does the parameter estimate. Figure 5.3 shows on the x-axis the correlation that was present between the input signal and the noise, as it entered the system, for different experiments. The y-axis shows the 2-norm on $(\theta - \theta_0)$, the obtained parameter vector minus the true parameter vector. From this figure can be deduced that biased estimates are more likely to occur when a high correlation is present.

The recursive output error method seems to give the best (statistical) results. And also with respect to the other tests it performs very well. This makes it a valuable method. Moreover, it is recursive and consequently demanding less computing power and storage. Although this last argument does not necessarily hold when only short data sequences are considered.

With respect to a control objective, all methods make a good estimate of gain margin and

phase margin. Except for the Dual Youla Method. This is probably due to the high order estimate of the plant. A model reduction step was already mentioned to be necessary, but lies outside of the scope of this project. From Figure 5.2 can be concluded that the obtained model fails, if it were used for a pole-placement controller design.
The two-stage method performs well. It can be easily implemented using the standard open-loop identification algorithms that are provided by the MATLAB Identification Toolbox. Although classical identification methods were not considered in this report, it must be mentioned that the two-stage method fits in the framework from these methods. In [Van der Klauw (1995)] the direct, indirect, joint input-output and two-stage method are merged into one General Identification method.
With respect to the identification for control method, some remarks can be made. First of all, it performs quite well. After the first iteration the control performance error is already half of the initial one. In later iterations, it starts to oscillate. The fifth iteration has been taken as a final one. In this particular case, the loss increased a little after a sixth iteration. In practical situations, iterations are therefore executed until no further decrease of the control performance criterion is observed. The estimate of the model is given in Table 5.1. It is biased with respect to the true plant. This is not a problem, since it is the control performance error that is the criterion to be optimized. The application of the RθR Method to a 'real life' lab experiment will be discussed in the next chapter.
Some remarks must be made concerning the initial models that were used in the identification. Although a fair comparison demands the same initial model for all methods, different initial models have been used. The reason is that the Recursive Output Error has more stringent restrictions on the initial model than e.g. the Dual Youla Method. Moreover, the latter method constructs its own initial model from the knowledge of the controller. *Any* model that is stabilized by the controller can be used for the identification with this algorithm. The initial model for the Recursive Output Error method was adapted from [Landau (1996)]. However, this initial model did not give good results when fed to the RθR Method. It has therefore been slightly changed to make the RθR Method work as well.

VI

Magnetic Levitation

The theory introduced in the foregoing chapters has only been applied to simulated processes. The advantage of simulations is clear. Full control over the experimental conditions is possible and "what if" type of experiments can easily be carried out. However, the use of a "real life" system to test theoretical results is valuable. In this situation full control over the experimental setup is no longer possible. Noise and unmodeled dynamics can show up and introduce difficulties. The experiments that are described in this chapter were all carried out on a magnetic levitation process. The goal of this process is to position an iron ball using a magnetic force to compensate the gravitational force exerting on the ball. This process is schematically depicted in Figure 6.1(a). In the system under consideration the ball is to be suspended at a distance of ten to fifteen millimeters under an electromagnet. The next section will discuss a physical model of the system. Modelisation gives some idea of the properties of the system and the derived model can be used to tune some initial controller that stabilizes the system. The system setup gives rise to the implementation of a cascade control scheme. Control of the system and related topics will be discussed in the third section. The forth section will describe the experimental setup in more detail. Attention will be paid to the construction of the process and the implementation of the (discrete time) controller. The last two sections will be devoted to identification and identification for control.

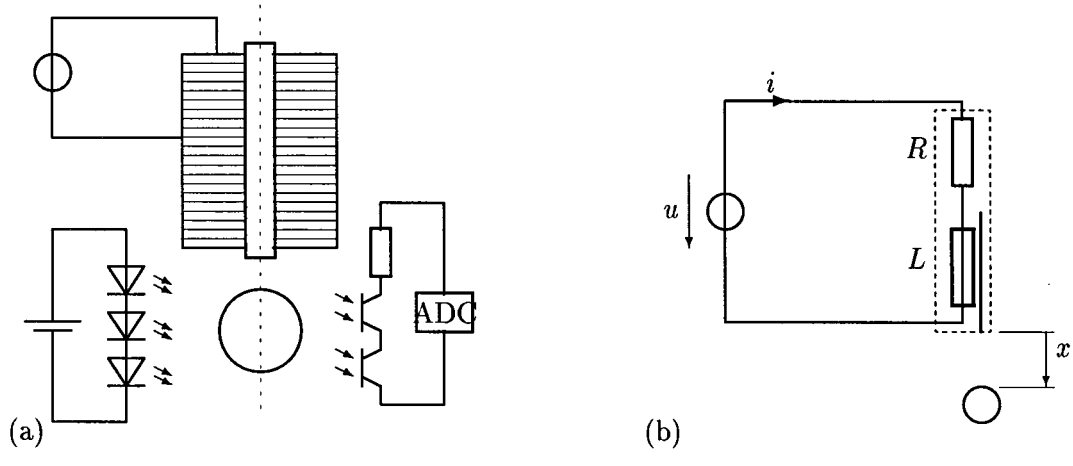

Figure 6.1: (a) Schematic experimental setup and (b) definition of symbols.

6.1 Physical modelisation

The modelisation of the system consists of finding the relations that link the output of the system to its input. In a first attempt the input will be taken to be the voltage, u, that is applied to the magnet. The position of the ball, x, is the output that must be controlled. From the more detailed description of the process, that is given in the next section, it can be found that also the current, i, in the magnet is available from measurements. Therefore the current will be considered to be an output as well. Consider Figure 6.1(a) and 6.1(b). The magnet can be modelled by a resistance and a perfect spool in series, leading to the following equation:

$$u = Ri + \frac{\mathrm{d}\psi}{\mathrm{d}t}, \tag{6.1}$$

where R is the Ohmic resistance of the magnet. The magnetic flux is represented by ψ. With regard to the equations of motion of the ball, the following relations are trivial:

$$m\ddot{x} = F_g + F_m \tag{6.2}$$

$$F_g = mg. \tag{6.3}$$

The gravitational force and the magnetic force are represented by respectively F_g and F_m. The mass of the ball is m, g is equal to the gravitational acceleration. An expression for the magnetic force can be found from the expression for the magnetic energy E_m, which is a function of the flux ψ and the position x of the ball,

$$E_m = E_m(\psi, x). \tag{6.4}$$

Under Assumption 6.0 the flux can be calculated from

$$\psi = Li, \tag{6.5}$$

where the inductance L depends on the position of the ball. This latter (static) relation will be derived empirically in the fifth section.

Assumption 6.0
In order to arrive at a physical model for the levitation process, the assumptions below with regard to the magnet will be made:

- The core does not have any flux of its own.
- The ball does not create any flux.
- There are no Foucault currents present.
- No hysteresis is present.
- There is no saturation.

□

The total differential of the energy can be found from equation (6.4),

$$\mathrm{d}E_m = \frac{\partial E_m}{\partial i}\mathrm{d}i + \frac{\partial E_m}{\partial x}\mathrm{d}x. \tag{6.6}$$

Further, the magnetic energy is equal to the sum of the electrical and mechanical work functions,

$$\mathrm{d}E_m = \mathrm{d}W_e + \mathrm{d}W_m, \tag{6.7}$$

where the two right hand side terms are

$$\mathrm{d}W_e = i\mathrm{d}\psi = iL\mathrm{d}i + i^2\frac{\mathrm{d}L}{\mathrm{d}x}\mathrm{d}x \tag{6.8}$$

$$\mathrm{d}W_m = -F_m\mathrm{d}x. \tag{6.9}$$

Subtracting equation (6.7) from (6.6) gives

$$0 = \left[\frac{\partial E_m}{\partial i} - iL\right]\mathrm{d}i + \left[\frac{\partial E_m}{\partial x} - i^2\frac{\mathrm{d}L}{\mathrm{d}x} + F_m\right]\mathrm{d}x. \tag{6.10}$$

Since the current i is independent of the position x, an expression for the magnetic force can now be found from:

$$\frac{\partial E_m}{\partial i} = iL \tag{6.11}$$

$$\frac{\partial E_m}{\partial x} = i^2\frac{\mathrm{d}L}{\mathrm{d}x} - F_m. \tag{6.12}$$

Integration of (6.11) gives

$$E_m = f(x) + \int_0^i iL\mathrm{d}i = f(x) + \frac{1}{2}Li^2, \tag{6.13}$$

where $f(x)$ is some function of the position.Substitution of (6.13) in (6.12) leads to:

$$\frac{\partial E_m}{\partial x} = \frac{\mathrm{d}f}{\mathrm{d}x} + \frac{1}{2}\frac{\mathrm{d}L}{\mathrm{d}x}i^2. \tag{6.14}$$

From (6.12) follows the expression for the magnetic force,

$$F_m = -\frac{\mathrm{d}f}{\mathrm{d}x} + \frac{1}{2}\frac{\mathrm{d}L}{\mathrm{d}x}i^2. \tag{6.15}$$

Since the magnetic force should be zero in the absence of a current, $\mathrm{d}f/\mathrm{d}x$ must be zero. Hence,

$$F_m = \frac{1}{2}\frac{\mathrm{d}L}{\mathrm{d}x}i^2. \tag{6.16}$$

Collecting equations (6.1), (6.2), (6.3), (6.5) and (6.16), a state space description of the model is

$$\dot{x} = v \tag{6.17}$$

$$\dot{v} = \frac{1}{m}\left\{\frac{1}{2}\frac{\mathrm{d}L}{\mathrm{d}x}i^2 + mg\right\} \tag{6.18}$$

$$\frac{di}{dt} = \frac{1}{L}\left\{u - Ri - v\frac{dL}{dx}i\right\}. \tag{6.19}$$

Notice, that

1. The current is a state space variable that appears quadratic in the equation for the acceleration,

2. The factor $\mathrm{d}L/\mathrm{d}x$ is still unknown.

Because of the geometrical complexity of the system it is not possible to derive an analytical expression for $L(x)$ from physical laws. Therefore an empirical approach was chosen. Taking $\dot{v} = 0$ in equation (6.18) gives

$$\frac{\mathrm{d}L}{\mathrm{d}x} i^2 = 2mg. \tag{6.20}$$

By measuring the current as a function of the setpoint, the next relation was fit to the data:

$$\frac{\mathrm{d}L}{\mathrm{d}x} = -\frac{L_1}{\alpha} \exp(-x/\alpha), \quad \alpha > 0, \quad L_1 \text{ constant.} \tag{6.21}$$

Hence follows

$$L(x) = L_0 + L_1 \exp(-x/\alpha). \tag{6.22}$$

The constant L_0 can be found from identification of the magnet. Experiments and results are described in appendix C.
Substitution of the last equation in the state space equations leads to the final model:

$$\dot{x} = v, \tag{6.23}$$

$$\dot{v} = \frac{1}{m}\left\{-\frac{L_1}{2\alpha} \exp(-x/\alpha) i^2 + mg\right\}, \tag{6.24}$$

$$\frac{\mathrm{d}i}{\mathrm{d}t} = \frac{1}{L_0 + L_1 \exp(-x/\alpha)}\left\{u - Ri + \frac{v}{\alpha} L_1 \exp(-x/\alpha) i\right\}. \tag{6.25}$$

6.2 Linearisation

In order to find a stabilizing controller, the model must first be linearized. The setpoint can be found by taking the left hand sides of the state space equations equal to zero, which gives

$$\bar{v} = 0, \tag{6.26}$$

$$\bar{i} = \pm\sqrt{\frac{2\alpha mg}{L_1} \exp(\bar{x}/\alpha)}, \tag{6.27}$$

$$\bar{u} = R\bar{i}, \tag{6.28}$$

where the setpoint of the position, $\bar{x}$ can be chosen arbitrarily. Denoting the deviation variables by a tilde, the linearized state-space model is given by:

$$\dot{\tilde{x}} = \tilde{v} \tag{6.29}$$

$$\dot{\tilde{v}} = -\frac{L_1 \bar{i} \exp(-\bar{x}/\alpha)}{\alpha m}\tilde{i} + \frac{L_1 \bar{i}^2 \exp(-\bar{x}/\alpha)}{2\alpha^2 m}\tilde{x} = a\tilde{i} + b\tilde{x} \tag{6.30}$$

$$\frac{\mathrm{d}\tilde{i}}{\mathrm{d}t} = \frac{1}{L_0 + L_1 \exp(-\bar{x}/\alpha)}\tilde{u} + \frac{-R}{L_0 + L_1 \exp(-\bar{x}/\alpha)}\tilde{i} + \tag{6.31}$$

$$\frac{L_1 \bar{i} \exp(-\bar{x}/\alpha)}{\alpha\left(L_0 + L_1 \exp(-\bar{x}/\alpha)\right)}\tilde{v} = c\tilde{u} + d\tilde{i} + e\tilde{v}. \tag{6.32}$$

$a\left[\frac{m}{sA}\right]$	$b\left[\frac{1}{s}\right]$	$c\left[\frac{A}{sV}\right]$	$d\left[\frac{1}{s}\right]$	$e\left[\frac{A}{m}\right]$
12.95	1954.81	23.10	-38.81	-2.99

Table 6.1: Numerical values of the parameters of the transfer functions in the Laplace domain, for a setpoint $\tilde{x} = 15mm$.

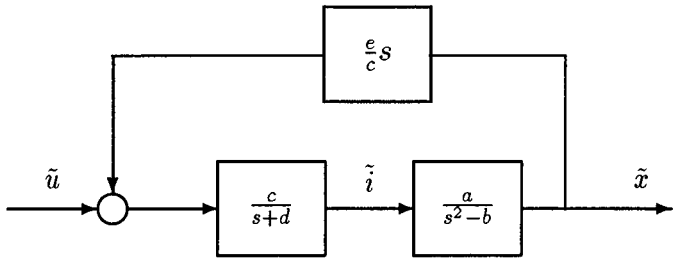

Figure 6.2: Interactions between state space variables in the Laplace domain.

The equivalent system in the Laplace domain is given in the Figure 6.2, where the numerical values from the parameters a to e can be found in Table 6.1 The counter reaction e represents the induced tension originating from the movement of the ball. Its effect is negligeable. The remaining interactions can be written in transfer functions in the Laplace domain:

$$G_1(s) = \frac{\tilde{i}}{\tilde{u}} = \frac{c}{s+d}, \tag{6.33}$$

$$G_2(s) = \frac{\tilde{x}}{\tilde{i}} = \frac{a}{s^2-b}. \tag{6.34}$$

The poles of the latter transfer function are $\pm\sqrt{b}$, which shows that the system is unstable. Notice furthermore that the overall transfer function $G_1(s)G_2(s)$ is of third order.

6.2.1 Cascade control

In the experimental setup that was used for the experiments both the position of the ball and the current in the magnet were available from measurements. This lead to the idea of cascade control. The control scheme is depicted in Figure 6.3, where K_1 and K_2 are controllers. The reference input is $\tilde{r}$ and the input signal was the current $\tilde{i}$[1]. In this control scheme, the controller K_1 is used to control the first order process $G_1(s)$. This process is stable and a high gain proportional controller eliminates the dynamics of this system. The controller has been implemented by analog devices. The process described by $G_2(s)$ however cannot be controlled by a proportional controller, since it pushes both poles of the transfer function away from the imaginary axis. The system can be stabilized by adding a derivative action to the regulator. The outer loop regulator was implemented on a computer.

[1] In the experimental setup only a tension could be applied to the magnet. A (known) resistance has been used to convert the current to a voltage.

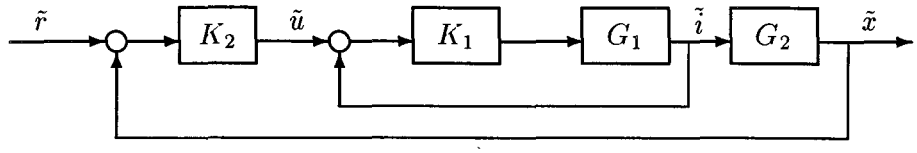

Figure 6.3: Cascade control scheme for the magnetic levitation.

6.2.2 Conversion to the discrete time domain

The outer-loop controller was implemented on a computer, and all relevant signals are sampled. It is therefore necessary to consider the discrete-time domain equivalent of the transfer function.

$$H_2(z) = \frac{\tilde{x}}{\tilde{i}}. \tag{6.35}$$

Then

$$H_2(z) = \mathcal{Z}\left\{\mathcal{L}^{-1}\left\{G_2(s)\right\}\right\}. \tag{6.36}$$

This is equal to

$$H_2(q^{-1}) = \gamma \frac{q^{-1}(1+q^{-1})}{1-\beta\, q^{-1}+q^{-2}}. \tag{6.37}$$

The sampling time is denoted by T_s. The numerical values of the parameters are for a sampling time of 10 ms,

$$\beta = 2.20, \tag{6.38}$$

$$\gamma = 0.65. \tag{6.39}$$

$$\tag{6.40}$$

The position is assumed to be measured in millimeters. This discrete time model was used to build a PD controller. Although various efforts have been done, it was not possible to tune the PD controller such that it stabilized the plant. However, by trial-and-error it has been possible to construct one. And this controller has been used in the identification experiments.

6.3 Identification

The identification of the plant can be exploited from the data that were obtained from measurements on the controlled process. Since the controller is of first order and the structure of the model is known. The fact that the order of the controller is lower than the order of the plant prevents the bias elimination least squares method (BELS) from being used for the identification of the plant. Also the two-stage method proved inapplicable. The reconstruction of the input signal may work fine, but this leaves the second step with an identification with two bounded signals. Therefore, the identified plant will always be stable, in contradiction to reality in the experiments. This leaves only the Dual Youla transformation and the recursive output error method to be used for identification.

6.3.1 Input signal

A multisine input signal has been selected that consists of ten sinusoids. This was necessary for the open-loop identification of the whole closed-loop that was used to construct a data filter. The design of the filter will be discussed below. The shape, and phase selection for a multisine of ten sinusoids was already given in Chapter 3. The Crest factor that was obtained from the Schroeder phase selection is equal to 1.92.

6.3.2 Model structure

Figure 6.3 shows that the plant is operated under cascade control. The transfer function of the inner loop can be taken equal to one. This leaves the plant G_2 under controller K_2. Defining the input to be the current, $u = \tilde{i}$ and the output the position of the ball, $y(t) = \tilde{x}(t)$. For notational convenience the tildes will be eliminated below. The plant is defined by two coprime polynomials $B(q^{-1})$ and $A(q^{-1})$ as

$$G_2 = \frac{B(q^{-1})}{A(q^{-1})} \tag{6.41}$$

According to the discretisation from the physical model, the following model structure has been chosen:

$$\mathcal{M}: \begin{cases} G(q^{-1},\theta) &= \frac{B(q^{-1},\theta)}{A(q^{-1},\theta)} = \frac{b_1 q^{-1}+b_2 q^{-2}}{1+a_1 q^{-1}+a_2 q^{-2}}, \\ y(t) &= G(q^{-1},\theta)u(t) + H(q^{-1},\theta)\epsilon(t) \end{cases} \tag{6.42}$$

where $G(q^{-1},\theta)$ represents the unknown plant and $H(q^{-1},\theta)$ defines the noise filter. In this model structure, the order of the numerator and denominator polynomials are equal to two. Later, it will be shown that order three polynomials sometimes give better results. The parameter vector consists of the parameters of the plant. The noise model will not be estimated and assumed to be equal to one. Evidence for this assumption is given below, where the identification of the closed-loop characteristic polynomial shows that the dynamics of the noise model can be neglected.

6.3.3 Construction of a prefilter

A first experiment was done with a multisine input signal. The data from this experiment were used by the RθR scheme to identify the plant. Although the estimate led to a model that was stabilized by the controller, the estimated plant turned out to be stable! In some cases, the estimated plant was unstable, but a newly designed controller did not stabilize the plant. Although different pole placements were chosen for the controller design, it was not possible to make the RθR scheme work.

A solution to this problem was found in a data filter. By filtering the data over an appropriate filter the identification was shown to work much better. The construction of this filter was done from an open-loop identification of the characteristic polynomial from signals in the loop. Notice, that the closed-loop itself contains the same "data filter". However, it turned out to be necessary to filter the signals directly before the identification.

The following equations, that are valid for the modelled closed-loop setup, were found to be useful in constructing the filter. Moreover, they include a validation in itself, since the closed-loop characteristic polynomial should be equal in both (estimated) transfer functions.

$$u = \frac{AS}{A_c} r - H\frac{AS}{A_c}\epsilon \tag{6.43}$$

and with $e = r - y$,

$$e = \frac{AR}{A_c} r - H \frac{AR}{A_c} \epsilon. \tag{6.44}$$

The identification of these two relations will be referred to as u-r and e-r identification. The closed-loop characteristic polynomial is denoted by A_c and is equal to $AR + BS$. This model represents a Box-Jenkins structure. Since the noise filter was not physically modelled, no information on the orders of H is present. The multisine input signal makes it possible that up to twenty parameters are estimated. To estimate the influence of the noise model, for both identifications a Box-Jenkins model structure is assumed, Define $\mathcal{A}$ as a model for A_c and $\mathcal{D}$ as a model for the denominator of the noise model of fourth order. From (6.43) and (6.44) it can be expected that $\mathcal{A}$ and $\mathcal{D}$ have the same dominant roots. The identified poles are given in Table 6.2. From this data can be concluded that an ARMAX structure is sufficiently

	$\mathcal{A}$	$\mathcal{D}$
$u - r$	-0.99	$0.41 \pm 0.84i$
	$0.70 \pm 0.46i$	$0.69 \pm 0.59i$
$e - r$	-0.67	$0.36 \pm 0.42i$
	$0.60 \pm 0.66i$	$0.70 \pm 0.43i$

Table 6.2: Identified poles of the plant and noise model in a Box-Jenkins structure.

complex, since the dominant poles in $\mathcal{A}$ and $\mathcal{D}$ are approximately equal.

In an ARMAX model structure, the plant model and the noise model are assumed to have the same poles. These (identified) poles are given in Table 6.3. The complex roots from both estimates are approximately equal, which gives confidence in the procedure. The data filter was constructed from the average:

$$L = \frac{1 - q^{-1}}{(1 - 0.7816 + 0.4138iq^{-1})(1 - 0.7816 - 0.4138i)}. \tag{6.45}$$

The derivative action in the numerator can be included to remove a possible offset on the data. The Bode plots of the data filter where the numerator was chosen equal to one are depicted in Figure 6.4

	poles	
u-r	$0.7974 \pm 0.4137i$	0.0523
e-r	$0.7659 \pm 0.4104i$	-0.8323

Table 6.3: Poles from ARMAX estimate of the system.

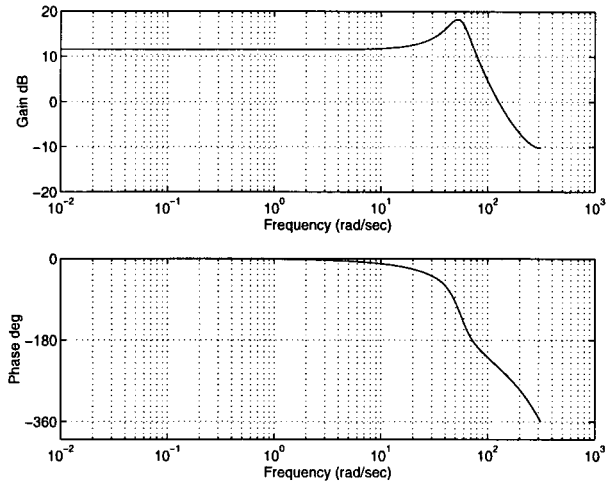

Figure 6.4: Bode plots of the data filter.

6.3.4 Data preparation

Consider an output error model structure for the magnetic levitation. Then, the closed-loop transfer function for the true system is:

$$y(t) = \frac{TB}{AR + BS}\, r(t) + \frac{AR}{AR + BS}\, e(t). \tag{6.46}$$

This implies that an ARMAX model structure is an appropriate model structure:

$$\mathcal{M}: \quad Dy(t) = Nr(t) + Q\epsilon(t). \tag{6.47}$$

Consider equation 6.37. Define the fixed factor in the numerator as $B_{fix} = (1 + q^{-1})$. A comparison of the true system and the model leads to

$$AR + \gamma\, q^{-1}\, B_{fix} S = D. \tag{6.48}$$

Since D is a polynomial that can be constructed from the estimates of the closed-loop poles (see subsection 6.3.3) and the controller polynomials S and R are known, γ and A can be computed from equation (6.48):

$$\hat{G} = \frac{0.26 \cdot 10^{-3}(q^{-1} + q^{-2})}{1 - 2.16\, q^{-1} + 1.09 q^{-2}}. \tag{6.49}$$

Most importantly, this analysis shows a factor 10^{-3} in the numerator. The order of magnitude in the numerator is 10^{-4} compared to the denominator. In order to make a proper identification, this problem should be easily eliminated by scaling the data.
Summarizing, the data should be preprocessed before any identification experiment can be carried out. Here, preprocessing consists of three steps:

1. Remove an average or trend from the data
2. Scale the data
3. Filter the data by a prefilter

Rec. Output Error	$\hat{G} = \frac{0.43q^{-1}+0.43q^{-2}}{1-2.47q^{-1}+1.13q^{-2}}$
Dual Youla Method	$\hat{G} = \frac{0.31q^{-1}-0.09q^{-2}-0.07q^{-3}}{1-2.82q^{-1}+2.46q^{-2}-0.68q^{-3}}$

Table 6.4: Identified models.

Method	2-norm validation	Poles of plant	Computed closed-loop poles
Recursive Output Error	0.0188	1.87 0.60	0.8810 $0.5733 \pm 0.5079i$
Dual Youla Method	0.0031	1.42 0.82 0.58	$0.8306 \pm 0.2718i$ 0.4365 0.4365

Table 6.5: Validation by sum of squares and pole placement.

6.3.5 Results

This subsection describes the results from the identification experiments, where the dual Youla method and the (filtered) recursive output error method were used. The modelisation gives rise to a second order model for the plant. Then, four parameters are to be estimated and a double-sine input signal is a sufficient excitation. However, the output error method then estimates a unstable plant and an unstable closed-loop. The dual Youla method works, but the 2-norm on the error is high (≈ 0.4). The same bad results are obtained with input signals of three and ten sinesoids. The correlation test that was carried out on the model from the dual Youla method gave a correlation of 0.6. The better results were obtained a *third* order estimate of the plant transfer function under the dual Youla method. The data was filtered over the data filter that was constructed above.
The recursive output error method was implemented in the "filtered" version. The data filter that was constructed above proved to work counterproductive and was therefore omitted. The identified model was of *second* order. This results show clearly that the identification procedure is a mathematical one. Although the physical modelisation led to a second order model, a better estimate is obtained with a third order approximation, if the dual Youla method is applied. The numerical values of the estimates are given in Table 6.4. A validation of the models will be discussed in the next section.

6.3.6 Validation

Dominant closed-loop poles

The identification of the data filter gives a nice means for validation purposes. The dominant closed-loop poles are known, and with the knowledge of the controller, any estimated model can be validated from a comparison of these poles and the ones that can be computed from the estimated model. The results of this validation are displayed in Table 6.5 and in Figure 6.5.

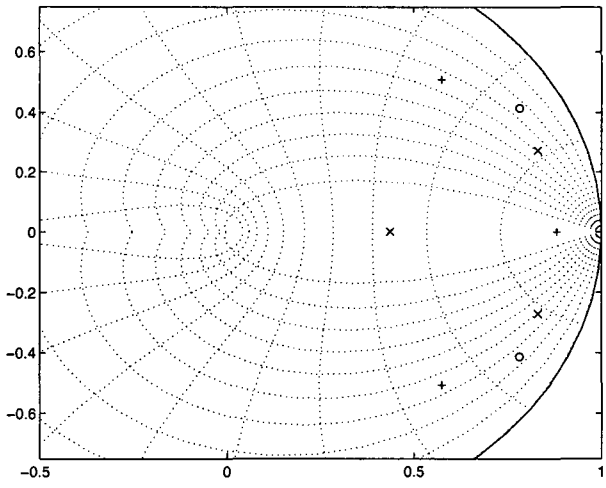

Figure 6.5: Validation of the dominant poles, (o) Experimentally identified poles from e-r and u-r identification, (x) identified by the Dual Youla Method, (+) identified by the Recursive Output Error Method.

Frequency domain validation

In the frequency domain, the Nyquist curves of the open-loop controlled plant (BS/AR) and the plant itself were identified. Section 4.6 introduced a means to find the Nyquist curve of a plant from closed-loop data. This method was applied to the magnetic levitation system and the primary results are gathered in Table 6.6 and Figures 6.7(a) and 6.7(b). The latter figure was constructed by employing the knowledge of the controller. It shows that the controller stabilizes the plant and that a reasonable gain margin is present in the system. This could be expected, because of the robustness of the PD controller. The identified cross-over frequencies were validated by a spectral analysis of the data. However only few data were available (the system becomes unstable rapidly for bigger α) a spectral analysis can confirm the identified cross-over frequency. The error margin in the spectral estimate of the crossover frequency is due to the small number of data that were used. Figure 6.6 gives the oscillatory response of the system and the spectral density of the output.

6.3.7 Conclusions

From the two validations above some conclusions can be drawn. The validation on the dominant closed-loop poles indicates that the Dual Youla Method performs better than the Recursive Output Error Method. Concerning the frequency domain validation, however, it is hard to judge which method performs best. In figure 6.7 b) the Recursive Output Error method seems to give the better results. From the Nyquist plot of the plant can be concluded that the Dual Youla Method performs better. There are some aspects that could explain these results. The Dual Youla Method was applied to a third order model. It therefore has more parameters to estimate than the Recursive Output Error Method. Furthermore, the latter method is sensitive to the initial model. This arises from the stability condition that includes a SPR condition, see 5.1.4. Another aspect is the data filter. This filter was applied on the

α	K_s	ω_x ARX estimate	Spectral validation	$\hat{G}$	$\hat{G}C$
0.0	2.28	0.98	0.96 ± 0.05	-0.2978 +0.2192i	-0.4386 +0.0000i
0.0	2.51	1.02	1.03 ± 0.10	-0.2643 +0.1912i	-0.3984 +0.0000i
0.2	2.23	0.82	0.76 ± 0.05	-0.4123 +0.2185i	-0.4843 -0.0822i
0.2	2.25	0.83	0.82 ± 0.10	-0.4062 +0.2141i	-0.4809 -0.0823i
0.4	2.06	0.56	0.52 ± 0.01	-0.6510 +0.2209i	-0.5345 -0.1712i
0.4	2.10	0.58	0.54 ± 0.02	-0.6311 +0.2125i	-0.5276 -0.1733i
0.4	2.17	0.62	0.57 ± 0.05	-0.5397 +0.1780i	-0.4682 -0.1611i
0.5	1.18	0.34	0.33 ± 0.01	-1.4476 +0.3175i	-0.8971 -0.2857i

Table 6.6: Identification of the Nyquist curve of the magnetic levitation. $C = S/R$ is the controller.

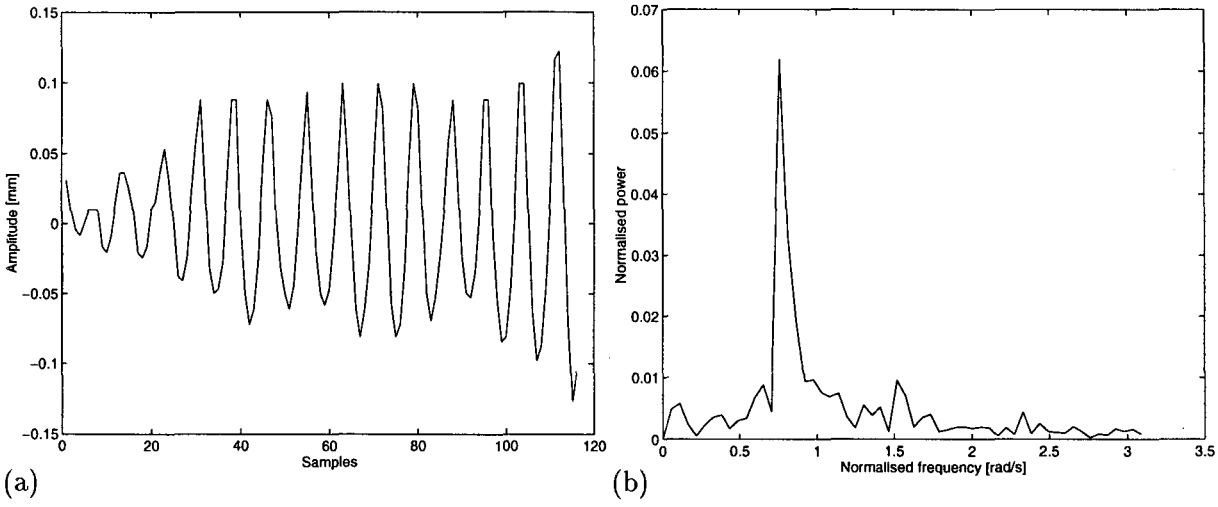

Figure 6.6: Typical example of the self oscillations (a), for $\alpha = 0$; (b) The power spectrum.

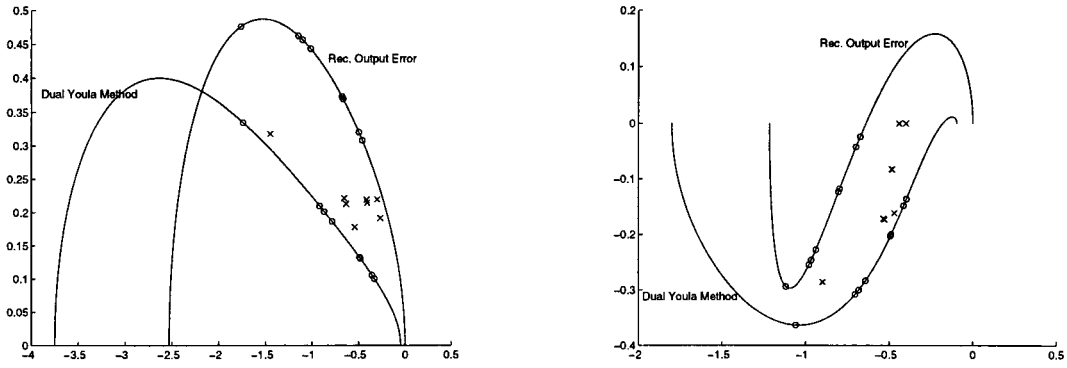

(a) (b)

Figure 6.7: (a) The identified Nyquist curve of the plant. (b) The estimated points on the Nyquist curve of the open-loop controlled system. The crosses denote the nonparametric Ziegler-Nicols estimates of the Nyquist curve. The circles denote the corresponding frequencies on the parametrically estimated Nyquist curves.

data that were fed to the Dual Youla algorithm. On the contrary, the Recursive Output Error Method did not work when the data filter was applied to the data. Again, this proves that the data filter contributes to a better estimate of the process.

6.4 Identification for control

The identification for control scheme was applied to different data sequences and a validation has been performed by a 2-norm criterion on the control error as defined in 5.91.

6.4.1 Setup for the identification

The model structure was chosen according to the physical modelisation:

$$\mathcal{M} \quad [1 + a_1\, q^{-1} + a_2 q^{-2}]y(t) = [b_1\, q^{-1} + b_2 q^{-2}]r(t) + \epsilon(t) \tag{6.50}$$

This model structure contains four parameters to be estimated. A complicated input signal is therefore not necessary. The experiments showed the better results with a multisine input signal, that consisted of ten sinesoids. Furthermore a square wave input signal has been selected for validation purposes. A data filter was necessary to obtain good results and has been implemented. It differs only slightly from the filter that was constructed above. The filter has three poles, at 0.77 and $0.75 \pm 0.45i$ and no derivative action was implemented. A scaling of the data was implemented for the reasons that were already mentioned. The designed poles of the closed loop were located at 0.4, 0.5, $0.65 \pm 0.4i$ and 0.75 in the complex plane. The number of poles (five) made a higher order controller necessary. The initial

Iteration	Poles of plant model	Dominant closed-loop poles
Initial	1.42 0.69	$0.77 \pm 0.42i$
1^{st} iteration	1.41 0.71	$0.79 \pm 0.36i$
2^{nd} iteration	1.31 0.70	$0.74 \pm 0.29i$
3^{rd} iteration	1.31 0.71	$0.78 \pm 0.29i$
4^{th} iteration	1.30 0.71	$0.77 \pm 0.29i$
5^{th} iteration	1.29 0.71	$0.69 \pm 0.22i$

Table 6.7: Poles of the model and the dominant closed-loop poles. These poles were identified by a coprime factor identification.

controller was a PD controller. Five iterations have been performed. The results and the validation are discussed below.

6.4.2 Results and validation

Since the goal of the RθR-scheme is the construction of a model-based controller, the scheme can best be evaluated by the control objective. Furthermore a validation with respect to the dominant poles of the closed loop has been carried out. Table 6.4.2 shows the poles of the estimated models and the identified closed-loop poles from a coprime factor identification, where the location of the dominant poles from the u-r and e-r identification were averaged. No dominant real poles were identified. Therefore the dominant closed-loop poles in tabel 6.4.2 should be compared with the designed dominant poles: 0.65 ± 0.4 and 0.75. Note, that the dominant closed-loop poles for the initial situation correspond to those that were computed in subsection 6.3.3. With regard to the identification objective, Figure 6.8 gives the control performance criterion for both the multisine input signal, that was used in the identification, and for a square wave input signal. The latter experiments were carried out exclusively for the purpose of validation. The numbers for the initial situation have not been included, since these numbers are determined by the first experimental setup and not a result from the RθR-scheme. As an example of the effectiveness of the scheme, a modelled output, the measured output and the control performance error are depicted in Figure 6.9. The controller of the second iteration has been used to construct the picture. Other evidence of the success of the RθR-method can be found from the tracking properties of the initial controller, and the controller that was constructed in the last (fifth) iteration. These are depicted in figure 6.10. The overshoot has decreased (notice the scales on the axes), as well as the oscillations.

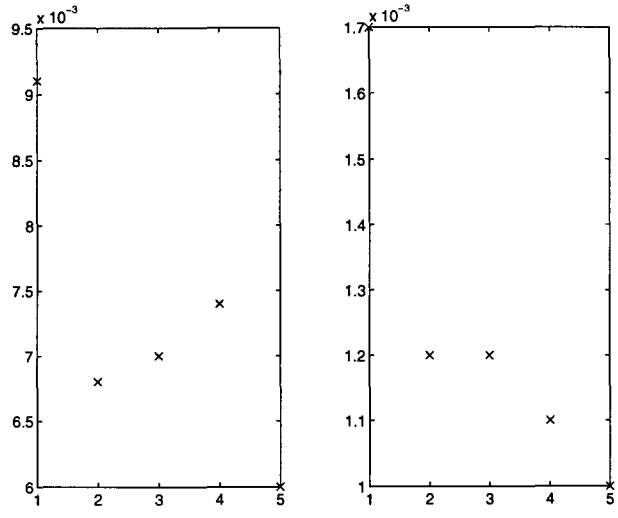

Iteration	Multisine	Square wave
1	0.0091	0.0017
2	0.0068	0.0012
3	0.0070	0.0012
4	0.0074	0.0011
5	0.0060	0.0010

Figure 6.8: Development of the control performance criterion for a multisine input signal (left) and for a square wave input signal (right).

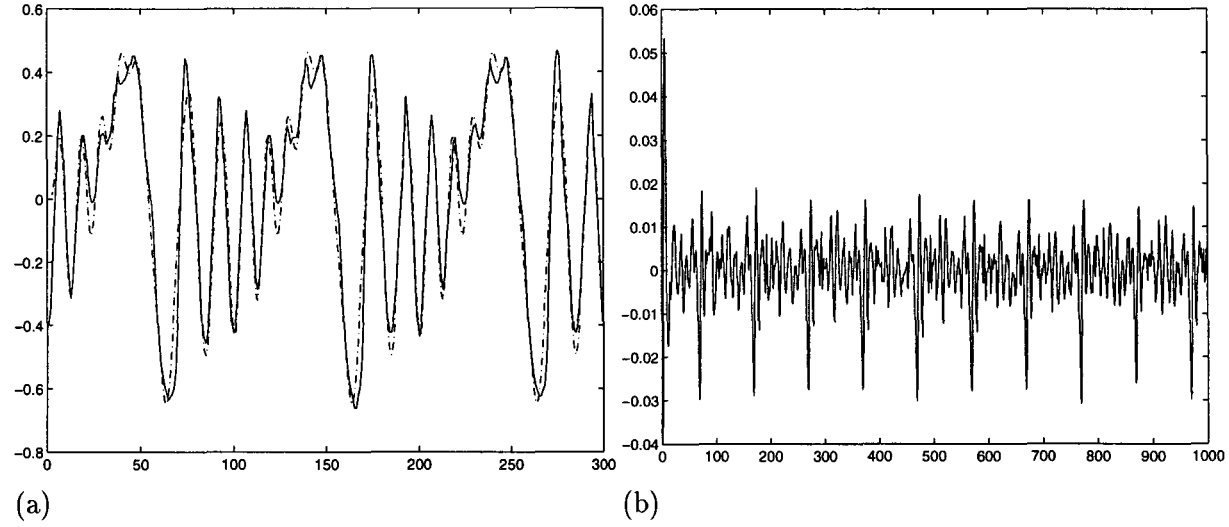

(a) (b)

Figure 6.9: (a) Measured (-) and desired (.-) output, (b) the control performance error.

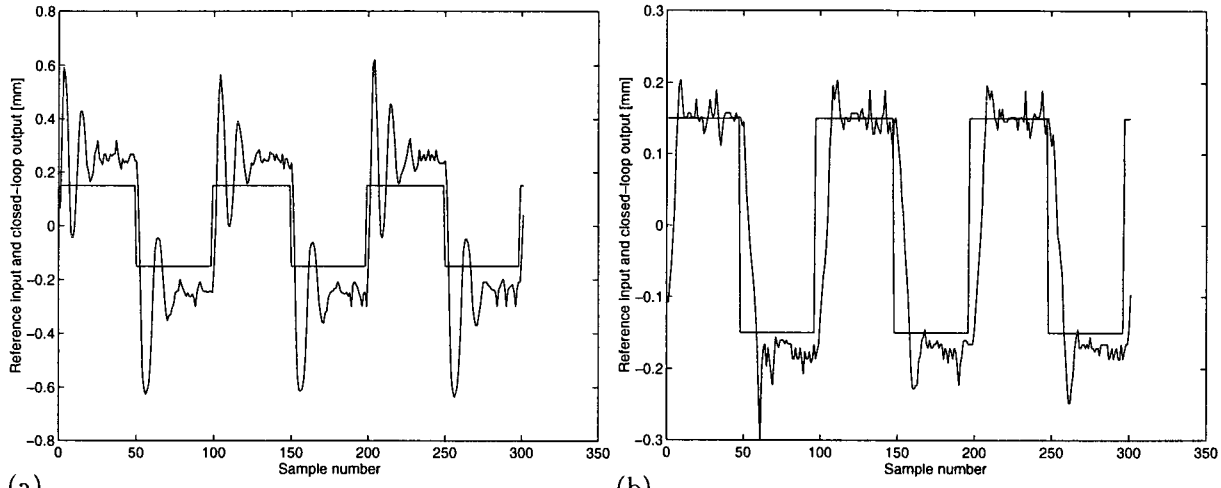

Figure 6.10: Tracking performance of the initial PD controller (a), and of the controller after five iterations (b).

VII

Conclusions and outlook

This chapter reviews the most important conclusions from this report. Moreover, it gives references to articles that appeared very recently and are interesting to mention, but were not considered within the context of this report.

7.1 Identification using finite data

The main difference between the "classical" closed-loop identification schemes and the algorithms that are discussed in this report is the goal of the identification. "Classical" methods aim at an identification , i.e. a reconstruction, of the true plant. Consequently, the system should be a member of the model set, $\mathcal{S} \in \mathcal{M}$. Recent algorithms, however, aim at a control objective. The identified model should be appropriate for model-based controller design and this respect, only the plant is to be identified, $G_s \in \mathcal{G}$, but $\mathcal{S} \notin \mathcal{M}$. The requirements that are met are

1. If $G_s \in \mathcal{G}$, but $\mathcal{S} \notin \mathcal{M}$, the estimate $\hat{G}$ must be consistent;

2. The model must be of low order, and hence it only *approximates* the real plant;

3. It should be possible to incorporate control design specifications into the identification procedure, if $\hat{G}(q^{-1}) \neq G_s(q^{-1})$.

Furthermore, the problem of finite data is addressed. "Classical" ,methods are of a "PEM nature", i.e. their consistency properties are only asymptotic. This also holds for the two-stage method. It was shown by [Van der Klauw (1995)] that this method can be incorporated in a general identification scheme, that further included the direct identification method, the indirect identification method and the joint input-output method.
The availability of only finite data also plays a role in the validation. A frequency domain validation of the estimated plant is not possible with short data records. The validation methods that were examined in this report can handle this restriction. Furthermore, they are also directed towards the control objective. The identification of the closed-loop characteristic polynomial proved an efficient way to capture the dominant closed-loop dynamics. Notice, that this validation is *controller dependent.*

7.2 The role of the initial model

The initial model proved essential for a successful identification experiment. The functionality of the identification algorithms that were reviewed in this project almost all depend on the initial model for the plant. The Recursive Output Error Method has the strongest restriction. The algorithm is assured to give a consistent estimate of the plant only, if a "strictly positive real" condition is satisfied. The Dual Youla Method is the easiest to handle in this respect. It constructs an initial model from the knowledge of the controller only. This made the identification of the magnetic levitation easy. It was much more difficult to construct an initial model for the Recursive Output Error Method. A detailed model from first principles was not a good candidate. And this model also turned out to be useless in the controller design. The initial model is not necessarily one of the plant. The BELS method needs an initial estimate of the closed-loop transfer function. However, it is difficult to give general guidelines on how to choose an initial model. During this project, the choice was sometimes "ad hoc". This was already mentioned in section 5.3. Further research on the choice of the initial model and its influence on the finally estimated model would therefore be a nice future expansion from this project.

7.2.1 Construction of the data filter

Another reason why it was so hard to identify the magnetic levitation process, was the noise. But in order to construct a proper data filter one needs a good model of the plant. However, an experimentally obtained noise filter proved to work fine. Therefore the following data preparation steps are proposed:

1. If an initial model is necessary, extract it from the closed-loop data.
2. Employ this knowledge to construct a data filter.

It was shown that this data filter is *essential* for the RθR Method to work on the levitation process. The Recursive Output Error Method is able to construct a data filter itself. It is therefore, that the "filtered" algorithm was used for the identification. Also the Dual Youla method that was used to identify the magnetic levitation process needed the data filter. Furthermore, a scaling of the data was essential. The difference in the order of magnitude in the numerator and denominator of the transfer function was of order 10^4. The identification has not successfully been carried out until this problem had been removed by a scaling of the data.
In chapter 5 it was mentioned that tackling the identification problem is sometimes rather an art than a method. This is clearly shown by the results from levitation experiment. Although the physical model is of second order, the Dual Youla Method gave the better results with a third order model structure. It is the *validation* that is essential in every identification experiment.

7.3 Identification for control

A new iterative identification for control scheme has been successfully applied to a lab experiment: the magnetic levitation process. In order to arrive at these results, a special real time Labview interface has been constructed to supervise the experiments. Also, an interface with

Matlab has been developed to make a transfer of data between the two software packages easy to handle. Furthermore, the Labview interface gives nice means to "play" online with the controller and other parameters of the process, e.g. the sampling time. It can therefore also be used for educational purposes. With respect to the experimental setup, one aspect was crucial. At first instance, the infra-red sensor was assumed to be linear. This difficulty had to be removed to make the experiments successful. The problem has been solved by a calibration of the sensor, and the implementation of the 'inverse' of the sensor in the software. During the experiments several problems were encountered. The construction of the data filter proved an essential step in the identification process. Furthermore, an appropriate input signal had to be chosen. A study of different input signals and some literature has been performed to arrive at a multisine input signal, that has been applied during all the experiments. A last step in the identification process was the design of a robust pole placement. This was not trivial and by trial-and-error one has been constructed. It turned out to work quite fine during the identification process.

7.4 Recent developments

By an example, this report shows that a closed-loop identification can give better results than an open-loop one. Recently, it has been shown [Hjalmarsson *et al.* (1996)] that a closed-loop identification gives a better performance than an open-loop identification, if the criterion is model based control. It is therefore preferable to perform the identification from closed-loop data, even if the system is stable and open-loop measurements are available.
With respect to the BELS Method, the major problem of this method has recently been removed. The restriction on the order of the controller has been removed. In [Zheng (1996)] it is shown that the method can also be applied to a system with a low order controller. The solution is the implementation of a stable digital prefilter, that can be used to augment the dimensions of the $\mathbf{M}$ and $\mathbf{H}^{\mathrm{T}}$ matrices, such that the restriction on the orders drops.

Bibliography

[Åström (1993)] K.J. Åström
Matching criteria for identification and control
Proc. 2nd European Control Conference, Groningen, pp 248-251 (1993).

[Bore-Kuen (1995)] L. Bore-Kuen
Closed-loop identification using the dual Youla control parametrization
Int. J. Control, Vol. 62, No. 3, pp 1175-1195 (1995)

[Godfrey (1993)] K. Godfrey (editor)
Perturbation signals for system identification, Prentice-Hall, England (1993).

[Guillaume *et al.* (1991)] P. Guillaume, J. Schoukens, R. Pintelon, I. Kollár
Crest-factor minimization using nonlinear Chebyshev approximation methods
IEEE Transactions on Instrumention and Measurement, Vol. 40, No. 6, pp 982-989 (1991).

[Guillaume *et al.* (1992)] P. Guillaume, R. Pintelon, J. Schoukens
Nonparametric frequency response function estimators based on nonlinear averaging techniques
Published by IEEE (1992).

[Hjalmarsson *et al.* (1996)] H. Hjalmasson, M. Gevers and F. de Bruyne
For model-based control design, closed-loop identification gives better performance
Automatica, Vol. 32, No. 12, pp 1659-1673 (1996).

[Van der Klauw (1995)] A.C. Van der Klauw
Closed-loop identification issues in the process industry. Dr. dissertation, Eindhoven University of Technology, Netherlands (1995).

[Landau (1996)] I.D. Landau, K.Boumaïza
An output error recursive algorithm for unbiased identification in closed-loop
Presented at the IFAC World Congress 1996 (july), San Fransisco.

[Ljung (1987)] L. Ljung
System Identification: Theory for the User, Prentice-Hall Inc., Englewood Cliffs, NJ (1987).

[Schoukens *et al.* (1994)] J. Schoukens, R. Pintelon, P. Guillaume
On the advantages of periodic excitation in system identification
SYSID '94 Copenhagen Denmark, Vol. 3, pp 153-158 (1994).

[Schrama (1992)] R.J.P. Schrama
Approximate identification and control design. Dr. Dissertation, Delft University of Technology, Netherlands (1992).

[Söderström and Stoica (1989)] T. Söderström, P. Stoica
System Identification, Prentice-Hall, Hemel Hempstead, UK (1989).

[Van den Hof and Schrama (1993)] P.M.J. van den Hof, R.J.P. Schrama
An Indirect Method for Transfer Function Estimation from Closed Loop Data
Automatica, Vol. 29, No. 6, pp 1523-1527 (1993).

[Van den Hof and Schrama (1994)] P.M.J. van den Hof, R.J.P. Schrama
Identification and Control - Closed Loop Issues
SYSID '94 Copenhagen Denmark, Vol. 2, pp 1-13 (1994).

[Zheng and Feng (1995)] Wei Xing Zheng, Chun-Bo Feng
A Bias-correction Method for Indirect Identification of Closed-loop Systems
Automatica, Vol. 31, No. 7, pp 1019-1024 (1995).

[Zheng (1996)] Wei Xing Zheng
Identification of closed-loop systems with low-order controllers
Automatica, Vol 32, No. 12, pp 1753-1757 (1996).

[Holmberg *et al.* (1996)] U. Holmberg, P. Myszkorowski and D. Bonvin
A Pole-placement Approach that Matches Identification and Control Objectives
Europeen Control Conference 1997, Brussels.

Samenvatting

Het ontwerp van een regelaar voor een bepaald proces is meestal gebaseerd op een model van het proces. Een analytische afleiding, waarbij wetten uit de natuurkunde en de scheikunde worden toegepast leidt soms tot een complex hogere orde model, dat niet geschikt is voor het regelaarontwerp. Een alternatieve aanpak is identificatie van het systeem. Deze aanpak maakt gebruik van meetdata om de parameters van een bepaald model te schatten. Het is bekend dat een identificatie op basis van meetdata uit een systeem *met* regelaar vaak de beste resultaten geeft voor het ontwerp van een nieuwe regelaar.
In dit verslag worden verschillende methodes onderzocht die het gesloten lus identificatieprobleem kunnen aanpakken. Het bevat een studie van zowel de grondslagen van identificatie in het algemeen, als van het doel van de identificatie. Recent ontworpen methodes zijn theoretisch en middels een toepassing op een magneetsyteem onderzocht. Een Labview gebruikersinterface is ontworpen om het proces te regelen en om meetdata te verzamelen. Een speciale interface is geïmplementeerd om een uitwisseling van gegevens met Matlab mogelijk te maken. Deze interface maakte het bovendien mogelijk om door de gebruiker ontworpen ingangssignalen, die in de Matlab omgeving zijn gemaakt, in de experimenten die met behulp van Labview zijn uitgevoerd, te gebruiken.
Het succes van een identificatie experiment hangt in grote mate af van de keuze van het ingangssignaal. Verschillende ingangssignalen zijn bestudeerd en deze studie heeft geleid tot de conclusie dat multisinussignalen het meest geschikt zijn voor een identificatie experiment. Deze signalen bieden een volledige controle over de mate van excitatie en zij kunnen worden geoptimaliseerd naar informatiedichtheid.
Iedere identificatie moet worden afgesloten met een validatie. In dit verslag worden verschillende manieren om deze validatie uit te voeren bekeken. Dit overzicht bevat zowel een statistische validatie als een validatie die gericht is op het regelaarontwerp.
Speciale aandacht gaat uit naar het doel om een regelaar te bouwen op basis van het geschatte model. Een methode die iteratief een identificatie uitvoert en een regelaar ontwerpt is opgenomen in het verslag. Deze methode is toegepast op een gesimuleerd systeem en op het laboratoriumexperiment.
De experimenten hebben geleid tot een belangrijke conclusie. Alle identificatie methodes en het iteratieve schema hadden een datafilter nodig om tot goede resultaten te komen. Een methode om dit filter te ontwerpen op basis van meetdata uit een gesloten lus experiment is ontworpen en is succesvol toegepast op het magneetexperiment.

Appendix A

Åströms Example

The most important properties of Åströms example are given in this appendix. The system is defined as:

$$\mathcal{S} : G_s(q^{-1}) = \frac{q^{-1} + 0.5q^{-2}}{1 - 1.5\,q^{-1} + 0.7q^{-2}}, \tag{A.1}$$

with a sampling time equal to one. The poles are located at $0.75 \pm 0.37i$. The noise model was adopted from [Van den Hof and Schrama (1993)] and is of third order;

$$H_s(q^{-1}) = \frac{1 - 1.56\,q^{-1} + 1.045\,q^{-2} - 0.3338q^{-3}}{1 - 2.35\,q^{-1} + 2.09\,q^{-2} - 0.6675q^{-3}}. \tag{A.2}$$

The Bodeplot of this noise filter is given in figure A.1.
In the closed-loop setup, the following RST controller was implemented:

$$R = 1 - 0.6283\,q^{-1} - 0.3717q^{-2}, \tag{A.3}$$

$$S = 0.8659 - 1.2763\,q^{-1} + 0.5204q^{-2}, \tag{A.4}$$

$$T = 1. \tag{A.5}$$

The resulting closed-loop poles are $0.63 \pm 0.17i$. The Nyquist plot of the open-loop controlled system, i.e. $\frac{BS}{AR}$ is depicted in figure A.2. The Recursive Output Error Method works under the assumption that the transfer function R/A_c is strictly positive real (SPR), where A_c is the characteristic closed-loop polynomial. Figure A.3 shows that this is the case in this example.

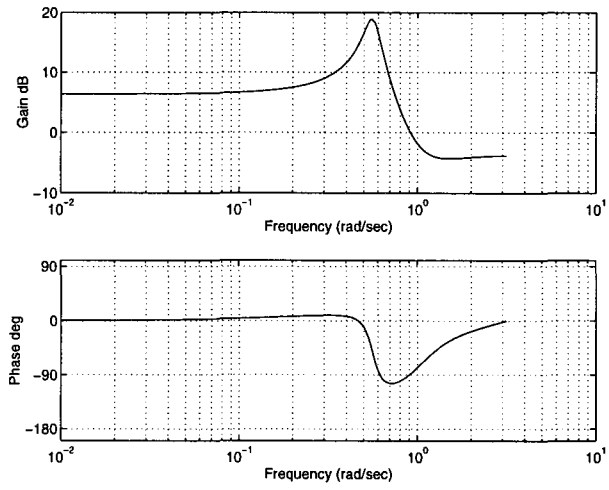

Figure A.1: Bode plot of the noise filter.

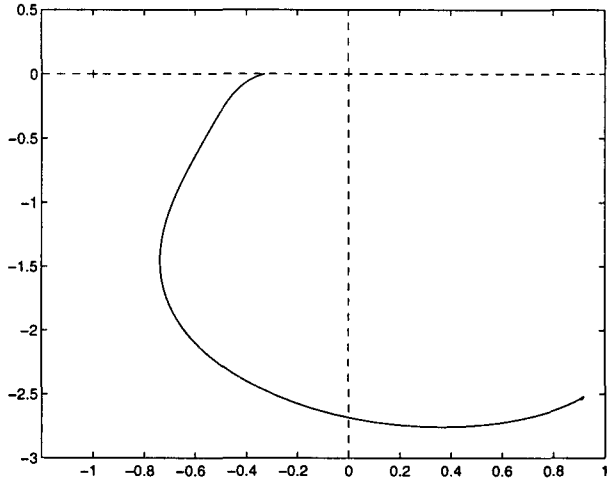

Figure A.2: Nyquist plot of the open-loop controlled system.

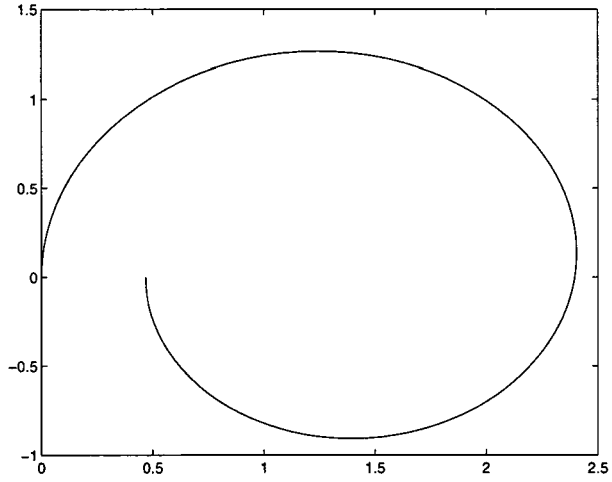

Figure A.3: The SPR condition is fulfilled in this example.

Appendix B

Mathematics

B.1 Matrix Inversion lemma

Suppose that **A** and **C** are nonsingular matrices (not necessarily of the same dimension) and **B**,**D** are such that $\mathbf{A}+\mathbf{BCD}$ exist and is nonsingular. Then

$$(\mathbf{A}+\mathbf{BCD})^{-1} = \mathbf{A}^{-1} - \mathbf{A}^{-1}\mathbf{B}\left(\mathbf{DA}^{-1}\mathbf{B}+\mathbf{C}^{-1}\right)^{-1}\mathbf{DA}^{-1}, \tag{B.1}$$

with $\left(\mathbf{DA}^{-1}\mathbf{B}+\mathbf{C}^{-1}\right)$ guaranteed to be nonsingular.

B.2 Computation of the Crest factor from a sampled signal

The Crest factor can be calculated from a continuous time signal $u(t)$ by

$$CF_u = \frac{l_\infty[u]}{l_2[u]}, \tag{B.2}$$

where l_∞ denotes the Chebyshev norm of the signal $u(t)$ and l_2 is the 2-norm. In general, the l_p norm of a function $u(t)$ taken over the interval $[0,T]$ is given by:

$$l_p[u] = \left[\frac{1}{T}\int_0^T |u(t)|^p dt\right]^{1/p}, \quad p \geq 1. \tag{B.3}$$

For large values of p this also defines the Chebyshev norm,

$$l_\infty[u] = \max_{t\in[0,T]} |u(t)|. \tag{B.4}$$

These definitions are valid for continuous time signals only. However, if the sampling is done at equally spaced time intervals and if the signal is a trigonometric polynomial, then $L_p[u_n] = l_p(u)$ for even values of p and for a number of measurements N is greater or equal to $pK+1$, where K is the order of the trigonometric polynomial. Notice, that since the Chebyshev norm is defined as a maximum the number of samples that is needed to calculate it is infinite. When only *finite* data are available, a lower bound of the Chebyshev norm is:

$$\|u\|_L = max_n|u_n| \tag{B.5}$$

The upper bound on the norm is

$$\|u\|_U = \frac{\|u\|_L}{1-K\pi/N}, \quad N > K\pi. \tag{B.6}$$

Proofs on this statements can be found in [Guillaume *et al.* (1991)].

Appendix C

Magnetic levitation

C.1 Open-loop identification of the magnet

From the theory in chapter 6 a first order model for the behaviour of the magnet has been derived. This model is given by:

$$\frac{\mathrm{d}i}{\mathrm{d}t} = \frac{1}{L_0}(u - Ri). \tag{C.1}$$

The voltage that is applied to the magnet is denoted by u, and is taken to be the input. The resulting current is denoted by i. The properties of the magnet, inductance and resistance are denoted by respectively L_0 and R. Defining $\alpha = R/L_0$ the transfer function in the Laplace domain is

$$G(s) = \frac{\alpha/R}{s+\alpha}. \tag{C.2}$$

Using a zero-order hold, the discrete time representation can be derived from:

$$G(q^{-1}) = \frac{1}{R}\mathcal{Z}\left\{\frac{1-\mathrm{e}^{-Ts}}{s}\frac{\alpha}{s+\alpha}\right\}, \tag{C.3}$$

$$= \frac{1}{R}\frac{\left(1-\mathrm{e}^{-\alpha T}\right)q^{-1}}{1-\mathrm{e}^{-\alpha T}q^{-1}}, \tag{C.4}$$

$$= \frac{bq^{-1}}{1+aq^{-1}}. \tag{C.5}$$

The sample time is T, and was 10 ms. From the constants a and b, the properties of the magnet can be derived:

$$R = \frac{1+a}{b}, \tag{C.6}$$

$$L_0 = \frac{RT}{-\ln(-a)}. \tag{C.7}$$

Since only two parameters are to be estimated a square-wave input signal is of sufficient order of persistence. The identification experiment has been performed and was validated by a statistical validation, by a mean square fit of the predicted output and by a comparison of the Bodeplot that results from the parametric model, and one that can be obtained by spectral analysis of the data. With respect to these criteria, the best results were obtained with an output-error model structure.

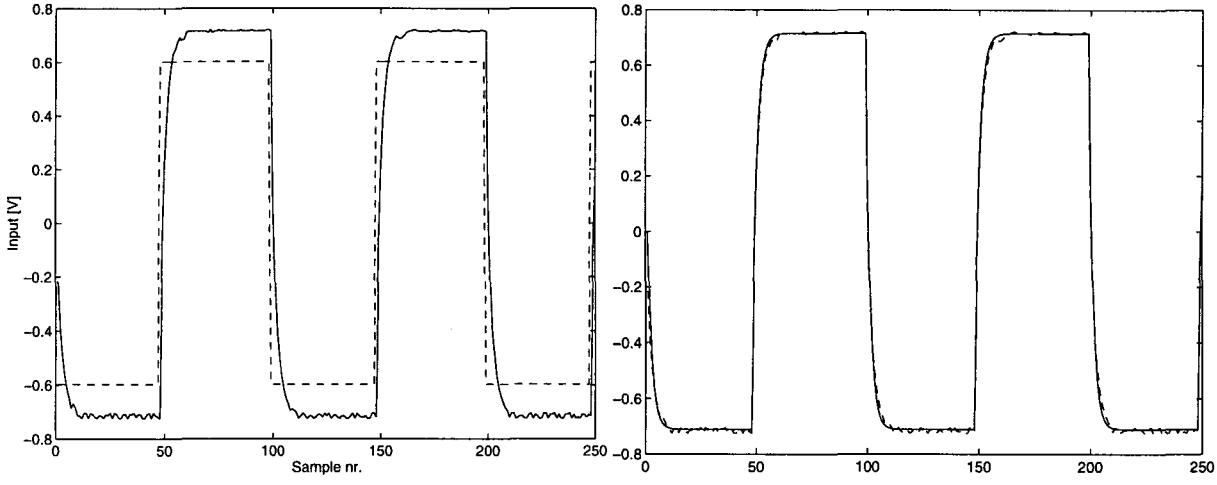

Figure C.1: Input-output data and the data fit.

Figure C.1 shows a part of the input-output data (the total number of measurements was 1024) and a comparison of the predicted output together with the measured output. Figure C.2 shows the bodeplots of both the parametric model and the nonparametric model. The coefficients a and b were estimated as: $a = -0.5974 \pm 0.0011$, $b = 0.2428 \pm 0.0007$. Hence, $R = 1.68\Omega$, $L_0 = 39mH$.

C.2 Determination of $\mathrm{d}L/\mathrm{d}x$

From the open-loop identification experiment, that was described in the section above, the properties of the magnet were calculated. Chapter 6 mentioned that the total inductance of the magnet not only depends on the magnet itself, but also on the position of the ball. The following relation was proposed to describe this phenomenon:

$$L(x) = L_0 + L_1 \mathrm{e}^{-x/\alpha}. \tag{C.8}$$

The determination of the constants L_1 and α will be described in this section.
Assume that the system of magnet and ball is controlled, such that the ball can be kept at a certain distance from the inductance. If only few disturbances are present, the input voltage applied to the magnet is nearly constant and so is the current in the magnet. From the derivative of C.8,

$$\frac{\mathrm{d}L}{\mathrm{d}x} = -\frac{L_1}{\alpha}\mathrm{e}^{-x/\alpha}, \tag{C.9}$$

and 6.20,

$$2mg = \frac{L_1}{\alpha} e^{-x/\alpha} i^2, \tag{C.10}$$

can be derived that:

$$\ln(i^2) = \ln\left(\frac{2mg\alpha}{L_1}\right) + \frac{x}{\alpha} = ax + b. \tag{C.11}$$

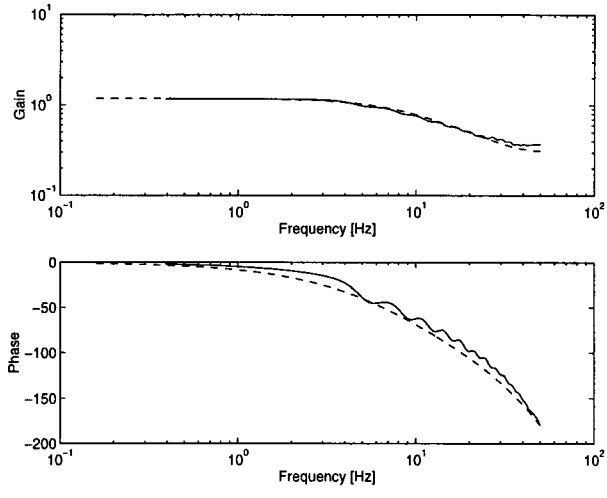

Figure C.2: Validation by Bode plots.

Then:

$$\alpha = \frac{1}{a}, \tag{C.12}$$

$$L_1 = 2mg\alpha e^{-b}. \tag{C.13}$$

The measurements that were carried out are depicted in the figures below. From these data was found that $\alpha = 5mm$ and $L_1 = 8.6mH$.

C.3 Calibration of the sensor

The sensor that measures the position of the ball is of an infra-red sensor. It consists of three LEDs and two photovoltaic sensors. This setup is depicted below. The characteristics, i.e. the voltage-position relation was in the first experiments taken linear. Later, it turned out to be necessary to calibrate the sensor and invert its characteristics. The measurements of the position of the ball and the resulting voltage on the sensors is depicted in figure C.5. A spline approximation was made, yielding the position of the ball for all measured voltages.

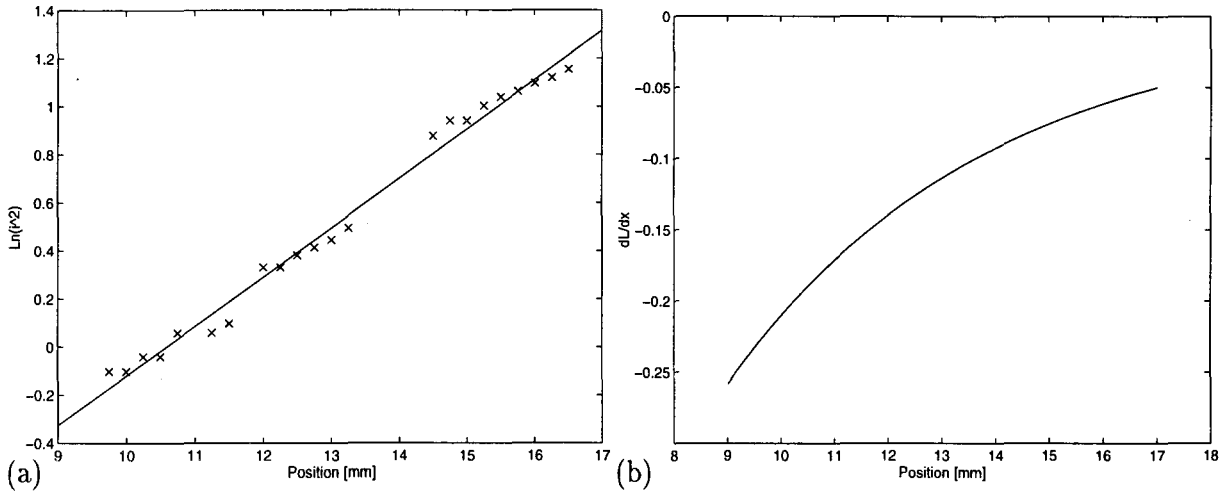

Figure C.3: (a)Measurement of $\mathrm{d}L/\mathrm{d}x$, (b) $\mathrm{d}L/\mathrm{d}x$ as a function of the position.

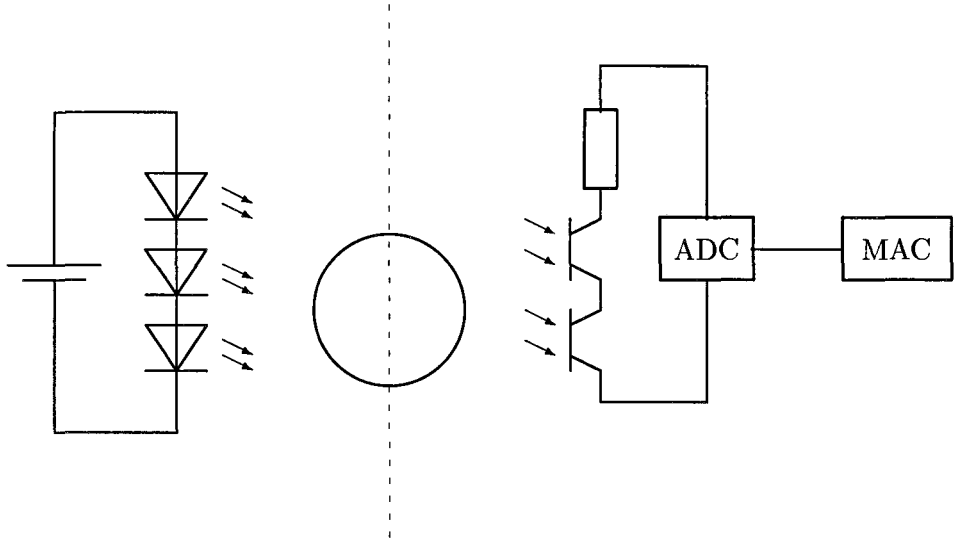

Figure C.4: The infra-red sensor (schematically)

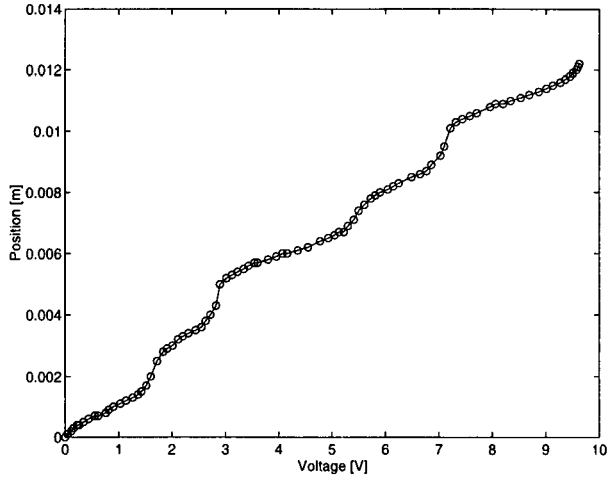

Figure C.5: Calibration of the sensor.